Journal of Environmental & Earth Sciences
https://journals.bilpubgroup.com/index.php/jees

REVIEW

Natural Drivers of Global Warming: Ocean Cycles, Anthropogenic Greenhouse Gases and the Question of Percentages

Peter J. Taylor

Independent Policy Analyst, Walton, Somerset BA16 9RD, UK

ABSTRACT

There is a widespread policy assumption that anthropogenic greenhouse gases are the main driver of the observed 1 °C rise in global surface air temperatures since 'pre-industrial' times. This paper demonstrates that the onset of the current warming trend began in the mid-19th century and is consistent with the rising phase of variable global warming and cooling cycles in both the Northern and Southern Hemispheres. Hemispheres. The last trough of the millennial cycle, the Little Ice Age, coincides approximately with the baseline of pre-industrial times used to calculate the impact of Anthropogenic Global Warming. Yet, half of the observed 20th century temperature rise occurred before 1950 when carbon dioxide levels remained low, with the remaining half happening at a similar rate of warming despite the much higher concentrations of greenhouse gases in the atmosphere. This study shows that when the amplitudes and rates of change of the long-term global cycles are considered, the anthropogenic component of warming can be reduced to 38% (using factors derived from the latest IPCC Working Group reports) to as little as 25% (using observational flux data of dominant Short Wave Absorbed Surface Radiation). These global climate cycles can be extrapolated into the future and the implications for policy of a large natural component to climate change are explored—in particular, the potential for mitigation strategies to have minimal impact and for the climate to cool consequent upon a cyclic down-phase.

Keywords: Global Warming; Ocean Oscillations; Natural Cycles; Environmental Policy

*CORRESPONDING AUTHOR:
Peter J. Taylor, Independent Policy Analyst, Walton, Somerset BA16 9RD, UK; Email: peter.j.taylor108@protonmail.com

ARTICLE INFO
Received: 4 November 2024 | Revised: 22 November 2024 | Accepted: 6 December 2024 | Published Online: 14 February 2025
DOI: https://doi.org/10.30564/jees.v7i2.7683

CITATION
Taylor, P.J., 2025. Natural Drivers of Global Warming: Ocean Cycles, Anthropogenic Greenhouse Gases and the Question of Percentages. Journal of Environmental & Earth Sciences. 7(2): 262–290. DOI: https://doi.org/10.30564/jees.v7i2.7683

1. Introduction

'If the dark side of concerns about Earth's climate is fear, the bright side is data' [1].

1.1. 'Unprecedented Changes' – The Background

Climate science has identified an approximate 1 °C rise in Global Mean Surface Atmospheric Temperature (GMST), during the past 165 years (**Figures 1** and **2**). It is widely assumed that most of this warming is anthropogenic (**Figure 1b**) and hence controllable by initiatives that limit emissions of Greenhouse Gases (GHG) [2, 3]. However, this supposition is not as readily supported by climate science as policy makers are led to believe. The latest report (6th) of the United Nations' Inter-governmental Panel on Climate Change (IPCC), Summary for Policy Makers [3] makes no further claim than the two previous reports [4, 5] - that 'most' of *the post-1950* warming is anthropogenic [3]. However, the pre-1950 human contribution is estimated only from complex computer models of the earth-ocean-atmospheric dynamic (**Figure 1b**) that cannot replicate the most basic and universal feature of climate, oscillation.

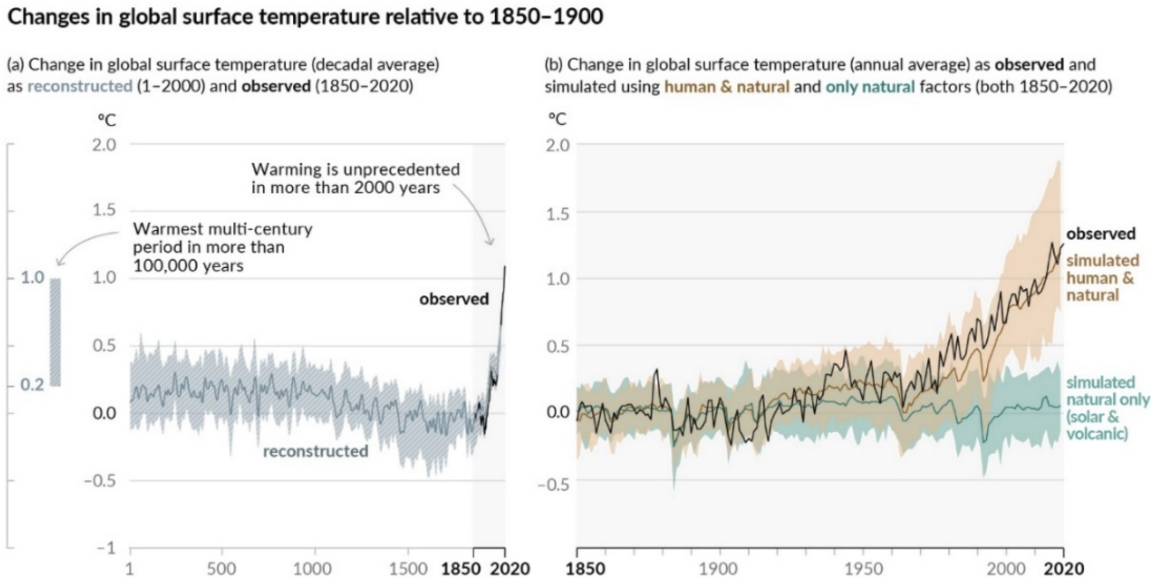

Figure 1. Observed and modelled temperatures. (**a**): reconstructed temperatures and observed instrumental data. (**b**): 1850∼2020 observed temperature and modelled.
https://www.ipcc.ch/report/ar6/wg1/chapter/summary-for-policymakers/FigureSPM2.

In the Summary for Policy Makers, the 6th Report of the IPCC states: 'The likely range of total human-caused global surface temperature increase from 1850–1900 to 2010–2019 is 0.8 °C–1.3 °C, with a best estimate of 1.07 °C'. This figure is derived by modelling the sum of the GHG positive forcing and assumed aerosol negative forcing and appears to match the whole of the observed global warming signal. However, the conclusion drawn is only that: 'It is very likely that well mixed GHGs were the main driver of tropospheric warming *since 1979*' (emphasis added) and of sea-level rise 'since 1971'. 'Main driver' is given as greater than 60% and 'very likely' encompasses a probability range of 66%∼90% [3].

Scrutiny of the modelled departure from natural variability (see **Figure 1b**) shows: a limited temperature range of −0.2∼+0.2 °C unchanging in amplitude over the 2000 years of the Common Era and throughout the 1850–2020 period. As so modelled, prior to 1950 GHG emissions have a minor effect (about 0.1 °C) in relation to natural variability. During this period there was a pronounced warming of about half of the centennial warming – a rise of approximately 0.5 °C not captured by the mean value of the model runs.

If we accept an IPCC figure of 60% anthropogenic for 'most' of the post-1950 rise and then add a potential 10% for the pre-1950 rise (see later discussion in Section 4.4), we can conclude from simple arithmetic that even within the range of IPCC estimates, the main driving force of warming since pre-industrial times is natural at about 60%.

However the IPCC graphics do not show *any* departure from the assumed natural variability of −0.2~+0.2 °C for the 1950~2020 period (indeed at year 2020, the mean of the computer runs shows no natural influence). Thus the whole of that rise would appear to be anthropogenic, contradicting therefore their own 60% consensus figure.

In the 6th Assessment Report (AR6), the limited range of long-term variability is held to include what the report now judges as relatively small perturbations of the former Little Ice Age/Medieval Warming Period (**Figure 1a**, grey shading). The report departs from previous reports in phasing out reference to the Little Ice Age/Medieval Warm Period, preferring one recent multi-ensemble modelling study of the past 2000 years, and assumes that multi-decadal cycles 'cancel each other out' in the longer term [3]: Figure FAQ: 3.2, chapter 3. The range of natural variability encompasses only multi-decadal variability attributable primarily to the Pacific Decadal Oscillation (PDO) and the Atlantic Multi-decadal Oscillation (AMO) [3]: chapter 3. pp. 446~447. The term 'variability' is preferred over 'oscillations' by the IPCC and there are no indications of 'cycles'. Indeed, the post-1950 attribution omits any reference to recovery from the recognised millennial cycle of which the Little Ice Age represented the most recent millennial trough, and once multi-decadal variability is accounted (i.e., the rise and fall cancels out) the residual trend is assumed to be entirely anthropogenic. This simulated natural component of the centennial record was presented as **Figure 1** at conference by Ramaswamy in February, 2019 (**Figure 1b**) [2].

There is no indication of a long-term repeating cycle. In place of cycles, IPCC adheres to selective use of proxy reconstructions that have not met ready acceptance within the paleoclimate community (Section 3.1). Here, evidence is presented from long-term ocean heat-content studies, as well as extrapolations from Antarctic ice-cores, that supports previous interpretations of a globally significant millennial cycle. This cycle can be expected to peak within the next three centuries, followed by a trough in the cycle. The societal significance of this cycle lies in its greater amplitude with increasing latitude, particularly in the Northern Hemisphere. The most likely mechanism for the long cycle and its constituent ocean oscillations (i.e., the cyclic storage and release of heat from the oceans) is a variation in wind patterns (Section 4).

With regard to modelling and attribution studies, it is noteworthy that Coupled General Circulation Models (in particular the suite of models derived from the Community Model Inter-comparison Project—CMIP, and used to underpin IPCC analyses), only began to track multi-decadal ocean oscillations in 2008. One modelling team predicted no further warming for a decade or more (which was borne out by a hiatus in surface temperatures extending to the year 2015)—see Section 4.2.

Discussion of the decadal removal of surface heat to the depth of the oceans began in the context of this recent fifteen year hiatus (from 1999~2014) [3]: chapter 3, p. 446. The IPCC 6th report highlights Pacific Decadal and Indian Ocean variability as the main cause of an 'hiatus' and of a very large release of heat from ENSO in 2015 that ended it. In this regard, one of the most recent treatments of heat-removal and ocean oscillations include predictions of several decades with no future surface warming [6]. With regard to centennial warming, surface station records (**Figure 2**) show that warming appears to begin around 1910, rises to 1940, flat-lines to 1975 (a previous hiatus) and then resumes to 2000 where it flat-lines again until the El Nino years of 2016~2024.

It looks as if the observed post-1950 warming rate has continued through the two decades of the 21st century – at approximately 0.14 °C/decade. However, the warming peak in 2016 of almost 0.5 °C above temperatures in 2015 was due in part to a major El Nino event and temperatures had receded by that same amount by 2021 as La Nina conditions recurred and persisted into 2023 [7] to be followed in 2024 with a resurgent El Nino.

Furthermore, the first half of the centennial record (from 1900~2000) shows a strong rise between 1920 and 1940 of 0.4~0.5 °C *at the same rate* as the later rise from 1980–2000. Yet, supposedly the latter period is mainly driven by anthropogenic greenhouse gas (GHG) forcing at a level five-times the previous concentration (Section 3). In this context, we briefly examine changes in radiative flux over the late 20th and early 21st century warming periods, finding a dominant Short Wave forcing compared to computed and measured fluxes of Long Wave radiation. There is evidence that there are long-term reductions in reflective cloud cover driving increased insolation that appear too large to be accounted for by AGW feedback mechanism (Section 4.4).

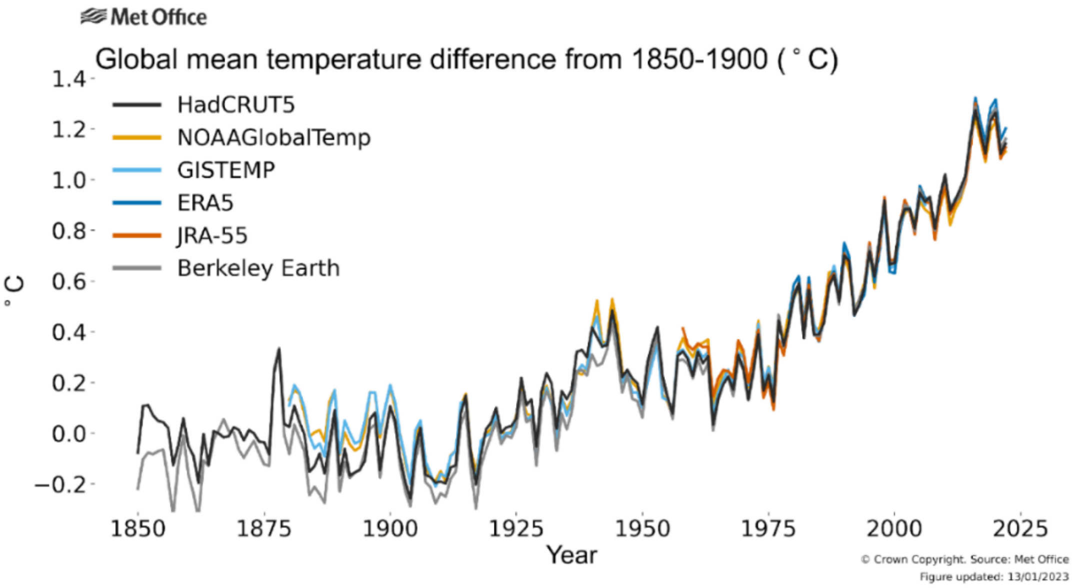

Figure 2. Global average surface temperature 1850~2022.
https://www.metoffice.gov.uk/weather/climate-change/what-is-climate-change.

At first, modellers assumed that human derived sulphur pollution was countering the carbon dioxide warming effect and models were adjusted to reflect an assumed aerosol component. However, surface-station radiation fluxes showed that global dimming to 1980 and brightening from 1980 to 2000 were primarily related to changes in cloud cover and natural aerosols, which produced over 4 W/m^2 of increased surface flux over the dominant global warming period (Section 4.4). The computed incremental effect of carbon dioxide over the same period is 0.3 W/m^2 (cumulative 0.98 W/m^2) – see **Table A1**, in the **Appendix A**. Human sources of sulphur pollution proved too local to have significant global effects [8–10]. Nevertheless, IPCC calculations lay great stress on the balancing effect of aerosols, despite a wide range of uncertainty (half-a-degree Celsius) [3], Figure SPM2].

1.2. Post-1950 Natural Variability

As noted for the post-1950 period, IPCC show no significant increase of natural variability above the pre-1950 range. However, when this period is examined in the context of a global recovery rate in ocean-heat content from the trough of a millennial cycle (Section 3.1), coupled with the known amplitudes of decadal and multi-decadal cycles, which peaked in the post-1950 period, (Section 2), the depiction of post-1950 natural variability as "limited" is questionable.

When asked at conference on this issue, Ramaswamy admitted that the IPCC models did not handle cycles at all well [2]. We therefore examine the neglected 'long cycle' of recovery from the trough of the Little Ice Age. A sustained rate of warming is evident in ocean heat content proxies beginning in 1850 and maintained at much the same rate in both halves of the 20th century [11–13]. Estimates of the centennial rate are of the order of 0.05 °C/decade (Section 3.1) and the data do not show any reason to dismiss a continued rate of change potentially contributing half of the post-1950 rise.

It is also shown from a brief examination of cloud changes and surface radiation flux (Section 4.4) that these factors out-weigh flux changes from the rise of anthropogenic GHGs. The issue as to how much cloud changes drive surface temperatures or the converse (i.e., are feedback to anthropogenic warming) remains open, but the conclusion remains that the sensitivity of the climate to anthropogenic GHGs has been over-estimated and in Section 5 we examine the implications with regard to predictions of future temperature rise.

1.3. Prediction and Policy

There are acknowledged uncertainties about the future evolution of GHG emissions and these contribute to varying scenarios of warming. However, future solar radiation changes may contribute, in particular UV effects on the Jetstream at times of reduced solar activity. In Section 5, we examine two models using GCMs for prediction of the effects of future reduced solar activity. We also examine the extrapolation of wave-forms derived from paleo-climatological studies, the instrumental surface-station record, tree-ring analysis, and the ice-core record, which contain two recent predictions of a natural cooling trend and examine these projections as potential counter effects to rising anthropogenic greenhouse gases. We briefly examine extensive work correlating solar activity cycles with surface temperature changes.

Finally, in Section 6, we look at the policy implications of a revised treatment of natural variability and climate cycles – where natural components can account for between 60% and as much as 78% (see Section 3.1.2) of the climate driving force.

2. Methodology

This review paper has six sections. Data sources are given where applicable in the reviewed papers. Evidence is reviewed in Section 3.1 for a long cycle that is variable at 800–1100 years in the late Holocene. The cycle has a similar amplitude (0.8∼1 °C) to the observed centennial global warming signal. It has its most recent trough in the Little Ice Age (ca 400 BP), and extrapolating from Antarctic cycles would be expected to peak within 3.3 centuries. In this respect, observational data is examined relating to the global rise in ocean heat content since 'pre-industrial' times, in particular the rate of warming of the oceans and transfer of heat to land [11–15]. Cycles of warming and cooling are identified in proxies from the paleo-climatology literature, including spectral analysis of ice-core records, lake sediments, ocean sediment cores and tree rings [16–26]. Section 3.2 reviews the evidence for multi-decadal and decadal oscillations peaking in the late 20th Century and relevant to claims of a dominant anthropogenic influence for this period, and relevant also to an observed 'hiatus' in the 21st Century. The amplitude and peaking points of these cycles are discussed, in particular, the limitations of global circulation models to adequately account for cyclic behaviour on millennial, centennial and multi-decadal timescales [23–34]. Section 4 explores mechanisms for natural cycles of warming and cooling, in particular the periodic storage and release of heat in the oceans [11–15] together with concomitant effects of cloud-cover changes as well as cycles of solar activity.

We consider estimates of the amplitude of multi-decadal cycles [16–21]. Evidence points to at least half the post-1950 warming being caused by natural cycles peaking during that period, and prior to 1950 only marginal effects of GHG emissions, thus indicating at least 60% dominance of natural forces over the centennial period. In Section 4.4, we consider evidence from radiation flux measurements, comparing measured surface flux of spectrographically resolved CO_2 radiation with satellite data on absorbed radiation, finding a potential 80% natural component of the driving force. In Section 5, we briefly examine modelled projections for the 21st century that incorporate a drop in solar activity associated with the Little Ice Age cycle [29, 30], as well as extrapolations of waveforms derived from paleo-climatological data [17, 19–21, 34]. Section 6 considers the policy implications of a dominant natural component to the warming pattern.

3. Ocean Cycles and Oscillations

3.1. The Long Cycle of 1000 Years in Ice-Cores and Tree-Rings

3.1.1. The Pre-Industrial Baseline and Treatment of Cycles in IPCC Models

The term 'pre-industrial' is widely used as a base-line from which to measure human influence on climate. Yet, that baseline also coincides with the most recent trough of a well-documented millennial cycle and the current apparently dominant anthropogenic influence coincides with the expected recovery phase of that cycle [16–22, 34]. This Holocene cyclical pattern reflects cycles during glacial periods with an average of 1500 years [17, 20, 21, 34] and which shorten to 1000 years during the later Holocene [20, 22, 31, 33, 34]. However, IPPC in its sixth report, claims that a combination of updated models, proxy-reconstructions and re-analysis of data sets has improved paleoclimatology, and although not explicitly stated, the millennial 'cycle' has disappeared to be replaced (again) by a 'hockey stick' (**Figure 1a**). Critics have been quick to point this out – for example, a coalition of scientists centred in the Netherlands with 1500 signatories – CLINTEL (https://clintel.org/).

Criticism is not confined to such 'grey literature' – twenty experienced paleo-climatologists co-authored a recent paper calling for a specialist working group at the IPCC to examine conflicting evidence and the potential bias within the IPCC in selecting specific reconstructions [35]. The controversy centres upon the weighting given in constructing the Global Mean Surface Temperature to equatorial regions where the perturbations evident in both the Northern and Southern hemisphere proxy data sets do not register strongly [36–38].

The relative stability of the equatorial regions thus make it an ideal marker for any unprecedented changes [36]. However, most industrial activity is located in the Northern Hemisphere land mass as well as key regions of global food production and surplus. Thus, fluctuation that impact upon high Northern latitudes are of great importance [32].

By focussing upon the equatorial regions, AR6 is claiming there is no significant global variability apart from the multi-decadal oscillations (variability is preferred to the terms oscillation and cycles) [3]: Figure FAQ: 3.2, chapter 3. Thus, with multi-decadal oscillations 'cancelling out' over a century according to IPCC, the 6th report does not address a long-cycle and in particular, recovery from the Little Ice Age

Hence, the 6th Assessment Report (AR6) arrives at the conclusion that anthropogenic emissions must have contributed 'most' (at least 60%) of the post-1950 rise, but why 'most' and not 'all' as **Figure 1** implies? Perhaps those responsible for the more cautious Working Group consensus position were not consulted on the graphic that surfaced in the Summary for Policy Makers, which relies upon the PAGESII consortium [38]. Furthermore, half of the global warming rise occurring prior to 1950 is clearly *within* natural variability – but the *modelled* runs do not adequately capture the substantial rise (half the centennial figure) from 1920–1940. The issue is presented here of long-term variability with regard to the previous millennia, including the Medieval Warm Period, the Roman Warm Period, the 'Antique' Little Ice Age that followed [35], and the most recent trough of the cycle, the LIA.

It may well be that such cold periods are not globally synchronous and spatially homogenous, but they are nevertheless variably periodic, and of great import for human society. Hsu (1998) identified five cold periods in this variable cycle across North and Central America, Europe and Asia at roughly 4000, 3000, 2200, 1000 BC, the post-Roman period in 4–6th century AD (300AD in China) and ending with the LIA (1275–1800 AD) [32]. Each coincided with the collapse of over-extended supply lines in the major empires of the time, together with drought, famine and mass migration. Bond Cycles (1997) identified similarly periodic ice-rafting events in the North Atlantic at 5900, 4200, 2800 and 1400BP [17]; and Buntgen et al. identify a following 'Antique' Little Ice Age commencing at 300CE (Common Era - AD) as well as the Little Ice Age at 1600 CE [34].

The global temperature amplitude of the most recent cold-to-warm period is clearly greater in the Northern Hemisphere, probably lying between 0.8 and 1.0 degree Celsius with larger regional extremes [35], whereas tropical ocean regimes may well lie within the plus or minus 0.2 °C in the IPCC graphic. The abandonment of the term 'cycle' and even 'oscillation' in the SPM downplays the societal significance of a repeating pattern. Recent studies support the global significance of millennial cycles [11, 20, 22] and whereas Buntgen et al. was published after the 6th assessment report, Davis et al. [19, 20] were available and not considered.

Several studies have undertaken spectral analysis of the long-term cycle pattern. Davis J.C. and G.C. Bohling [33] found cycles in temperature proxies in ice-cores throughout the Holocene of a 61-year and 950-year period identified from the GISP2 ice cores, and confirming the periodicity found by Bond et al. from ocean sediment studies [17]. The periodicities are further elaborated by Obrochta et al. [31], Yiou et al. [18], and Davis W.J. et al. for the Antarctic with teleconnection to the NH [20]. A 60-year global cycle was first identified by Schlesinger (1994) [23] and confirmed by Mazzarella and Scafetta [24]. Scafetta & Bianchini also identify through harmonic analysis a 980-year cycle in solar activity parallel to paleo-climate cycles of the same period, implying a solar driver (See Section 4.5 on External Mechanism).

In the Antarctic ice cores, peaks are identified at 750 and 1096 years together with several other frequencies corresponding to centennial and multi-decadal oscillations in the Antarctic Centennial Oscillation – ACO [20, 22], as shown in **Figure 3**.

A breakdown of temperature fluctuations in the Vostok ice-cores and wind-proxies for EPICA Dome C shows clear cyclicity [34]—see **Figure 4**. The wind cycle length shown here averages 1400 years matching the Bond cycle[17, 26] The cycle is variable: longer in the early Holocene and glacial records[31], and is composed of a centennial cycle shown to persist for at least 226,000 years, to summate and create the millennial cycle, and postulated to drive the NH cycles[20, 22, 34].

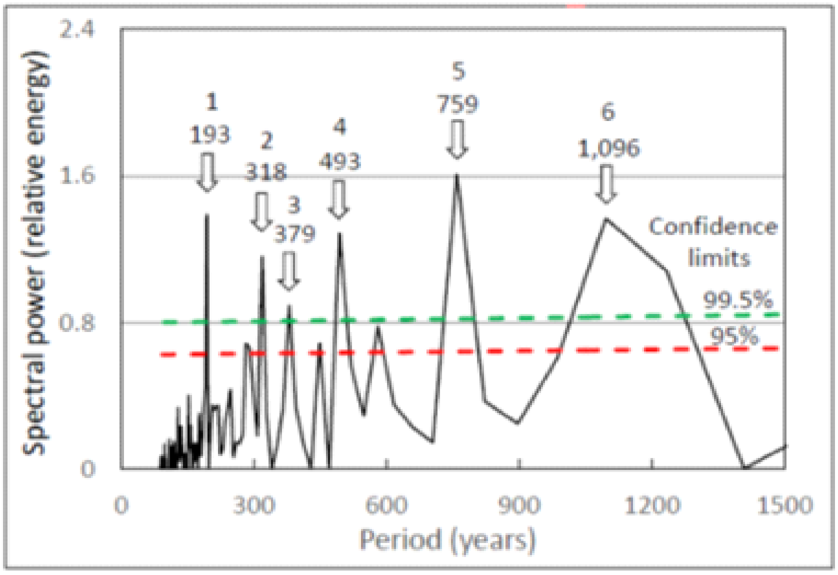

Figure 3. Spectral power density periodogram of temperature-proxy records from Vostok over the Holocene.

Note: Arrows and associated numerals designate spectral peaks at the indicated periods in years that are discernible at 99.5% confidence limits ($p < 0.005$). [Source: Davis, Taylor and Davis (2018)[20]: Figure 3, page 7.

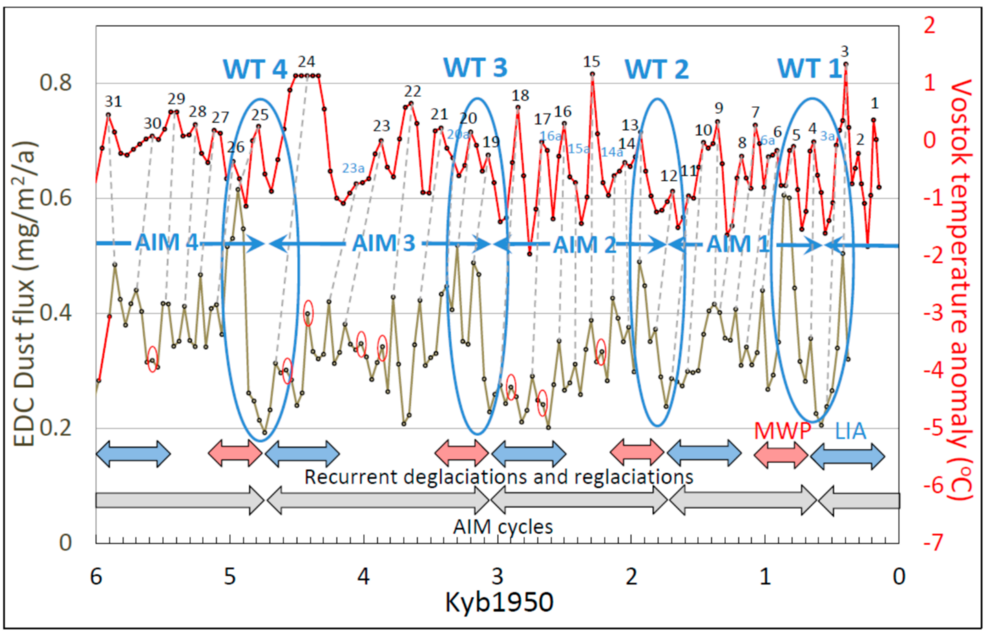

Figure 4. A millennial wind cycle in the Antarctic recent Holocene ice-core record.

From (Davis & Davis[34]: Figure 6): WT (Wind Terminus) 1–4 show termination points that mark the build-up of winds through the AIM (Antarctic Isotope Maximum) cycle and a steep drop at the end, usually followed by a steep rise in temperatures with amplitudes 2–3 °C. and an average period of 1400 years. Wind proxy dust data (lower grey curve) are from EPICA Dome C and temperature proxies (upper red) are computed from deuterium excess at Vostok. One-to-one matching (dashed lines) connect wind proxy peaks with corresponding temperature peaks, which are numbered according to the ACO/AAO cycle treated in Davis et al.[20, 22]. Red ovals enclose wind-proxy cycles that are unmatched in the temperature-proxy record. The red segment of the otherwise grey wind-proxy curve at 6000–5900 years before 1950 (Yb1950) denotes a period of missing data that was filled by interpolation for visual but not analytic purposes.

Spectral analysis confirms these periodicities but has limitations relating to non-stationary wave-forms. Yiou et al. (1997) confirmed significance by using several different methods, including multi-taper spectral analysis, singular spectrum analysis, maximum entropy method, principal component analysis, minimum bias spectral estimates and digital filter reconstructions[18, 25]. Yiou also noted a spectral peak at 10,000 years during the glacial cycles and it appears that the millennial cycles repeat within what may be a 10,000-year 'beat' cycle within the 100,000-year glacial cycle ([18], Figures 8 and 9, page 9).

3.1.2. Ocean Heat Content and the Long Cycle

Ocean heat content (OHC) is a better indicator of global warming and cooling patterns as 90% of the global warming signal is held in the ocean[3, 14, 15]. Many simulations of the post-industrial era are initialised at 1750 (and assume an equilibrium state), whereas Gebbie (**Figure 5**) explored an initialised simulation at 0015 CE in order to make the previous warming and cooling more visible[11]. Similar work on the profile of warming for the Pacific and the Atlantic showed that the deep Pacific still carried a signature into the LIA from the previous warm period (and hence the climate system was not at equilibrium), whereas the LIA cooling had penetrated to Atlantic deep waters[12]. Movement of surface-warmed water masses to greater depth would be expected to lower the rate of surface warming. **Figure 5** shows the rise and fall of the long cycle, and the 20th century rise in surface water temperatures from −0.3 ~ −0.2 to +0.6 °K. over 150 years to 2000 must be set in this context. The previous peak at 0.4 °K has an amplitude of 0.8 °K and this entirely natural peak follows the cold period identified by Hsu (and also Buntgen's 'Antique' Little Ice Age) as part of a series, and is reflective of cold periods (Bond Cycles) with similar periodicities from the glacial regime[17].

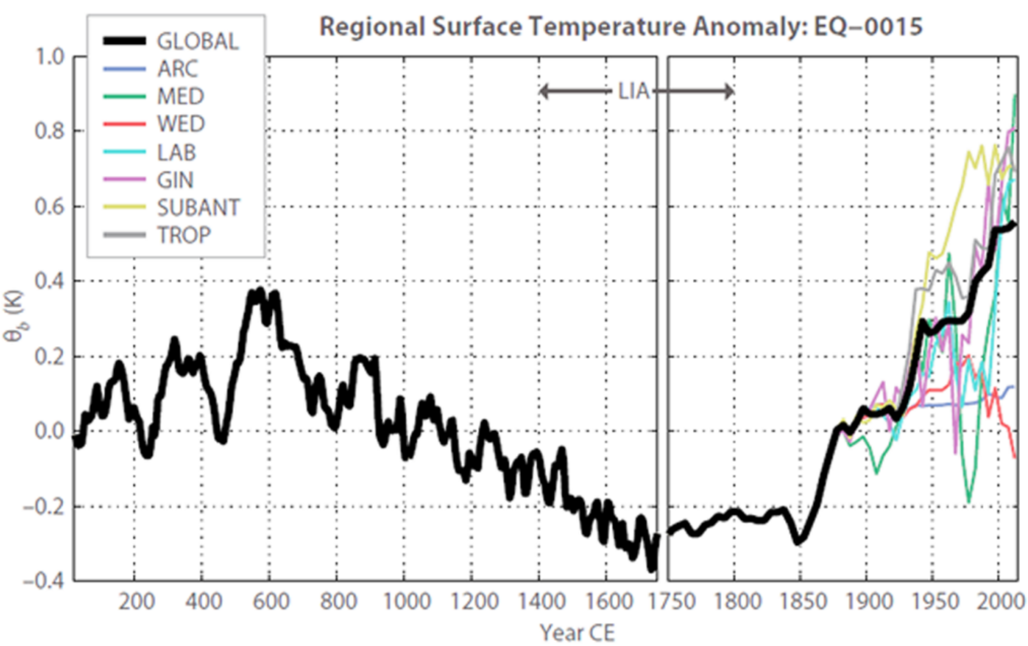

Figure 5. Reconstructed surface temperatures from simulations using blended paleo-oceanographic and instrumental data products[11, 12]. Note: the expanded time axis from 1750, and Surface temperature time series are relative to a baseline value at the year 15 CE (i.e., EQ-0015), including the global area-weighted average (black line) and seven major surface regions of the Atlantic sector (grey lines). Prior to 1870, the regional anomalies collapse onto the global mean. LIA = Little Ice Age. ARC = Arctic. MED = Mediterranean. WED = Weddell Sea. LAB = Labrador Sea. GIN = Greenland-Iceland-Norwegian Sea. SUBANT = sub-Antarctic region of the Atlantic. TROP = remaining subtropical and tropical regions of the Atlantic. CE = Christian Era.

This pattern of surface warming is mirrored by ocean heat content changes at depth ([11]: Figure 5) and the rise in heat content from 1850 is constant at about 10 Zettajoules/decade: 1850∼1950 and 11.5 ZJ/decade from 1950–2010. **Figure 5** shows that the current surface warming is about 25% (0.2/0.8 °K) beyond the previous natural global peak around 600CE It can also be seen that the period from 1920–1950, a period prior to the major acceleration of emissions, has the same rate or even a slightly steeper rise as the period from 1980–2000 when emissions were greater.

It can be argued that the 20th centennial rise is steeper than the rising phase of the previous warming and this may indicate effects from GHG emissions, however, when the 20th century is split pre-1950 and post-1950, the warming rates are identical despite the large difference (3x) in radiative forcing post-1950 from rising CO_2 levels.

Thus, the recent MWP/LIA pattern is part of a millennial series of cold and warm events of variable periodicity[18, 20, 22, 25, 33, 34] and displays a shortening that is obscured by averaging[31] and spectral analysis[20, 33]. This shortening will produce steeper slopes toward the end of a series, for example in the D/O and Bond cycles. This shortening of cycles is evident particularly in the Antarctic and Greenland ice-core data, where amplitudes increase and periods decrease toward the end of inter-glacials[20, 22, 34].

3.1.3. Recovery from the Little Ice Age – 1850 ∼2000

The CMIP suite of models[28] that is relied upon by the IPCC derives a limited surface temperature variability from 2000BP continuing through 1950 to 2020. The models include GHG changes due to land-use changes before the industrial era, but the major departure from this limited natural variability of +/−0.2 °C does not occur until after 1950 (**Figure 1**). The question thus arises as to the amplitude of the LIA cycle – as we saw from the critique of Buntgen et al.[35] and reply by Neukom[36] this amplitude will vary with latitude.

IPCC models thus show no apparent increase above their long-term variability as evaluated prior to 1950 when the centennial GSAT warming reached 50% of its value in 2000 (see **Figure 2**). The models' major departure in temperature above simulated natural variability occurs post-1950 and assuming the influence of GHGs shows, however, the same rate as observations for the 1920–1940 warming period despite the assumed dominance of greenhouse gas forcing during the latter phase.

Here it is argued that there must be a surface temperature recovery rate from the LIA. Gebbie's analysis shows recovery began around 1850 ([11]: Figure 2). In the **Table 1a** below, the global warming period as presented by Gebbie's data (**Figure 5**, Section 3.1.2) is split into several periods to examine the rates of change of temperature (note: Tss is reconstructed ocean temperature from **Figure 5**), as well as the concentration of carbon dioxide, the computed radiative forcing, and changes in ocean heat content.

There are key elements to the observed pattern:

1. The rate of global warming in the oceans begins well before the major emissions of CO_2 in the post-1950 era.
2. Global warming continues throughout the century at a steady rate of 0.05 °C/decade, as does the accumulation of heat in the oceans.
3. The rate of warming appears to increase in the period 2000∼2020 – but the increase comes after 2014 (following a 15 year hiatus) and is primarily due to a strong El Nino in 2016. However, the strong warming in 2016 (and even stronger in 2024—see Nikolov, Section 4.4, Figure 7) should not be used to derive short-term 'trends' as the warming will be followed by Nina conditions, and it is clear from the ASR data that increased insolation from cloud changes is driving the recent spike.
4. As shown in the **Appendix A Table A1** and **Figure A1**, the total change in the RF of carbon dioxide since 1750 is 1.4 Watts/m^2. Between 1750∼1850 it is 0.08 Watts/m^2 (ibid). The total RF in 2020 is 22.13 Watts/m^2 and the change since pre-industrial times is 6%, presumably all due to industrial emissions and land use changes. In terms of radiative effect, this change is very small (less than 1%) compared to the natural flux of SW radiation at the surface (approximately 240 watts averaged across the globe).

Furthermore, the rate of OHC change over the last century is monotonic and shows a near linear rise since 1920 (**Figure 5**), with the same rate maintained from 1971∼2010[11–13]. Thus, despite the increasing radiative forcing calculated for carbon emissions, the centennial rate of ocean warming shows no departure from the expected natural rate.

In Section 4.4 we compare the heat content rise of the order of 10 ZJ/decade which requires a surface flux of 0.47 W/m^{-2}/decade ([13]: Figure 14), to the computed and measured anthropogenic forcing. This latter totals 2.7 W/m^{-2} since 1750 (IPCC, Summary for Policy Makers, Figure SPM2), which includes all GHG gases and negative forcing from anthropogenic aerosols over the industrial period. At the turn of the millennium (2000∼2010), surface data show spectrally resolved RF for CO_2, at 0.2 W/m^2/decade for the 21st century[40].

These increments are fed into the complex climate models to derive subsequent future temperature increases – for example, the projected RF for a doubling of CO_2 in the suite of models used to inform the IPCC is 3.7 Watts/m^2 - to occur at about 2090 at current rates of emission. However, Shine[41], a key advisor to the IPCC, proposed a factor of 0.44 as a simpler guide. At the time, the models generated a factor of 0.88. The former would lead to a 1.6 °C rise by 2100, the latter to 3.2 °C —which is the mean of dozens of different model runs spanning a range of 2∼4.5 °C and the preferred approach of the IPCC.

However applying this factor of 0.44 to the ΔRF of 1.32 Watt/m^2 from 1900∼2020 (**Table 1a**) gives the same rate of observed temperature change since 1850 at approximately 0.05 °C/decade – hence the modeller's conclusion that carbon dioxide explains the whole of global warming. In contrast, the figures derived from oceanographic studies (**Figure 5**) show an observed decadal heating rate of 0.47 Watts/m^2 for most of the recovery phase of the long cycle[13]. This wattage at the surface is ultimately responsible for the long-term rise of 0.05 °C/decade in the proxy of ocean temperature. The observational reality would imply a factor of 0.1 instead of 0.44 for the simple conversion of RF to temperature. There is thus a clear need to examine the models and conversion factors of RF to temperature as well as the relation of stored heat to surface temperatures.

Table 1. (**a**) Time evolution of temperature, CO_2 concentration and radiative forcing 1850∼2020. (**b**) The period 2000–2024 using CERES calculations (from Nikolov, 2024, see Section 3.1.3).

(a)

Period	CO_2 ppmv	ΔCO_2 ppmv	ΔRF W/m^2	accRF W/m^2	ΔRF/decade W/m^2	ΔT^{ss} °C	ΔT/decade °C	ΔZJ (OHC)	Acc.ZJ	RF^{ss} W/m^2
1850–2000	285∼370	85	0.87	20.83∼21.7	0.005	0.8	0.05	75	625	
1900–1950	296∼313	17	0.19	20.96∼21.15	0.04	0.25	0.05	100	825	0.47
1950–2000	313∼370	57	0.56	21.16∼21.72	0.11	0.25	0.05	300	1075	0.47
2000–2020	370∼416	46	0.41	21.72∼22.13	0.20					

(b)

Period	ΔCO_2 (ppmv)	ΔRF (w/m^2)	ΔT°C	ASR (w/m^2)	ΔT/decade
2000∼2020	**370∼416**	**0.4**	**0.3**	**2.00**	**0.15**
2014∼2020	**392∼416**	**0.12**	**0.3**	**1.25**	**0.90**

Notes to the Tables:

Table 1a: The concentration of carbon dioxide derived from graphical displays according to the protocol described in (**Appendix A**), **Figure A2** and **Table A1**. The Radiative Forcing (RF) is derived from Modtrans calculations as described in **Figure A1** and **Table A1**. Figures for the change in Ocean Heat Content are derived from Giese[12] who also gives a figure for the net flux at the sea surface necessary to explain the accumulated heat (last column in **Table 1a** - RF^{ss}).

Table 1b: For the period 2000∼2020, temperature data are derived from Nikolov (See Section 3.1.1) as well as Absorbed Short-wave Radiation data available from CERES (see Section 3.1.1) for comparison. The change in the RF of CO_2 from 2014∼2020 is derived from Feldman's figure of 0.2 Watt/m^2/decade (noting this is a surface flux measurement).

A similar disjunction can be seen in the CERES data for 2000∼2024 (see Section 4.4) which identified roughly 0.5 Watts/m^{-2} as the net imbalance at the top of the atmosphere. However, the CERES measurements for the Top of the Atmosphere (TOA) have a wide margin of error and the 0.5 Watts/m^2 figure is derived by calibrating to the observed OHC data![42].

The question remains: if carbon dioxide levels cannot account for the pre-1950 rise of 0.4 °C, which in itself is half the centennial rise, and as stated by IPCC, CO_2 can account for only 'most' of the post-1979 rise but cannot account for the recent 2014∼2024 steep rise, then there is a pressing need to identify the dominant driver.

In Section 4.4, it is shown that the post-hiatus warming (2015∼2024) was driven by the natural ENSO cycle[43], concomitant cloud changes and greater surface insolation of up to 4x the aforementioned decadal increase of RF from carbon dioxide[40]. Similar arguments have been made for the 1980～2000 warming period using the ISCCP data sets on global cloud cover, and NASA's old FD data sets—showing that surface flux of short wave radiation dominates the forcing [44–46].

In conclusion, all of these data point to a very small (less than 1%) incremental effect of anthropogenic carbon dioxide on the natural flux of radiation at the surface. The natural flux is itself variable over at least decades and largely due to changes in cloud cover. When these cloud cover changes are quantified – as in the 1980～2000 ISCCP data, and 2000–2024 CERES data, the anthropogenic contribution is dwarfed by the Short Wave radiation flux changes – at about 75% natural and 25% anthropogenic.

3.1.4. A Pacemaker of the Global Millennial Cycle in the Southern Hemisphere

There have been claims that the LIA was essentially a regional and Northern Hemisphere phenomenon [47]. There are variations in timing across regions. However, North America and Eurasia have much the same timing and amplitude of temperature changes. Other low-frequency regional oscillations occur in the Southern Annular Mode that extend across South America and southern Australia, and show three periods of roughly 750 years peak-to-peak over the last 2400 years rising over the past 250 years towards a fourth modern-era peak [48–50]. Further, analysis of centennial cycles in the Antarctic ice-core – the Antarctic Centennial Oscillation (ACO), shows they summate to a millennial cycle, and points to a natural peaking toward the end of the 20th century [20, 22]. This southern hemisphere cycle which has been building over the last two centuries, correlates with wind proxy cycles determined from dust deposits in Antarctic ice-cores [34]. The ACOs build upon each other to form millennial cycles, i.e., the well-documented Antarctic Isotope Maxima (AIMs) found in ocean sediment data, and the peaks of the AIMs coincide with the peaks of the Dansgaard-Oeschger (D/O) oscillations in Greenland. The D/O build very rapidly compared to the AIMs and rise several degrees in a matter of decades. This teleconnection is well established though the mechanisms are not fully understood, and are thought to involve the Atlantic Meridional Overturning Circulation (AMOC) [51], which likely involves both atmospheric and ocean circulation responses to orbital cycles coupled with internal oscillators. These centennial, and perhaps also, millennial warming periods in the Antarctic are thought to be a consequence of cyclically stored heat surfacing and initiating changes in sea surface temperature, ice cover, wind patterns and precipitation, with the higher frequency cycles likely subject to an internal relaxation oscillator [20, 52]. The mechanisms of long-term heat storage and release are not fully understood, or quantified, but wind-driven resurfacing of heat in the Antarctic initiates global teleconnections, leading to the hypothesis that the warming and cooling periods in Antarctica are the pacemaker of global change [34].

3.2. Multi-Decadal Cycles

The millennial global cycle described in Section 3.1 contains higher frequency cycles from decadal to multi-decadal and centennial, which are variously described for regional seas and land masses. In the Antarctic, a centennial cycle averaging 350 years during glacial periods shortens during the Holocene to less than 100 years, producing an Antarctic Centennial Oscillation – ACO [20], also known as Southern Annular Mode – SAM which has global teleconnections [48–50]. Similarly, in the Northern Hemisphere the Arctic Oscillation [53–55] and the Atlantic Multi-decadal Oscillation (AMO) of approximately 80 years tele-connect [56–58], and in addition there are teleconnections to the Inter-decadal Pacific Oscillation – IPO, which combined with the AMO has been shown to influence global atmospheric patterns of wind strength, ocean heat storage and precipitation [59].

Variability of the AMO (and hence AMOC) is held to contribute not only to the recent slowdown in surface temperature rise (the hiatus from 2000–2015, see Section 4.2), but also to the cooling of the 1950–1975 period as well as the rise from 1980 to 2000 [59], and is potentially the main cause of the Arctic Oscillation [54, 55]. All of these inter-connecting regional cycles appear to produce the 60-year global signal present in spectral analyses of global temperature [21, 23, 24].

These higher frequency cycles ride upon the millennial wave pattern, raising or lowering its rate of change. It is thus important to place the latter half of the 20th century not only in the context of a peaking millennial cycle, but also the peaks and troughs of the multi-decadal cycles. Given that the decadal ENSO (at 3～4 years, with larger events at 10～15 years), affects global circulation patterns and global GSAT [60], it is to be expected that the multi-decadal oscillations of SAM, IPO, AMO and AO will have global effects on a similar scale, but observation-based estimates of their phase relationships and amplitude are elusive.

Some regional amplitudes have been estimated - for example, the Arctic Oscillation of 80~90 years with a regional amplitude of 2 °C. Polyakov et al. draw attention to how calculated rates of warming depend upon whether the time-periods capture this oscillation [53, 54]. For example, claims that the Arctic is warming much faster than the global average rate (3–4 times) generally do not take into account the previous peak in the 1930s. When the time period is extended to the full centennial warming, Polyakov and his team at the International Arctic Research Centre found the rates for the Northern Hemisphere and the Arctic are not statistically different at about 0.09 °C/decade and the concept of 'Arctic amplification' was not supported in data prior to the year 2000 [54].

The North Atlantic Oscillation (NAO) has been modelled as a predictor of mean northern hemisphere temperatures: Li et al. [61] sought to derive the residual Northern Hemisphere Temperature from the effects of the AMO/NAO and their analysis shows that the AMO can explain the whole of the de-trended NHT and by implication, at least half of the NHT rise (**Figure 6**). Their model predicted a decadal fall in NHT from 2012 (not accounting for ENSO effects or the trend in GHG emissions).

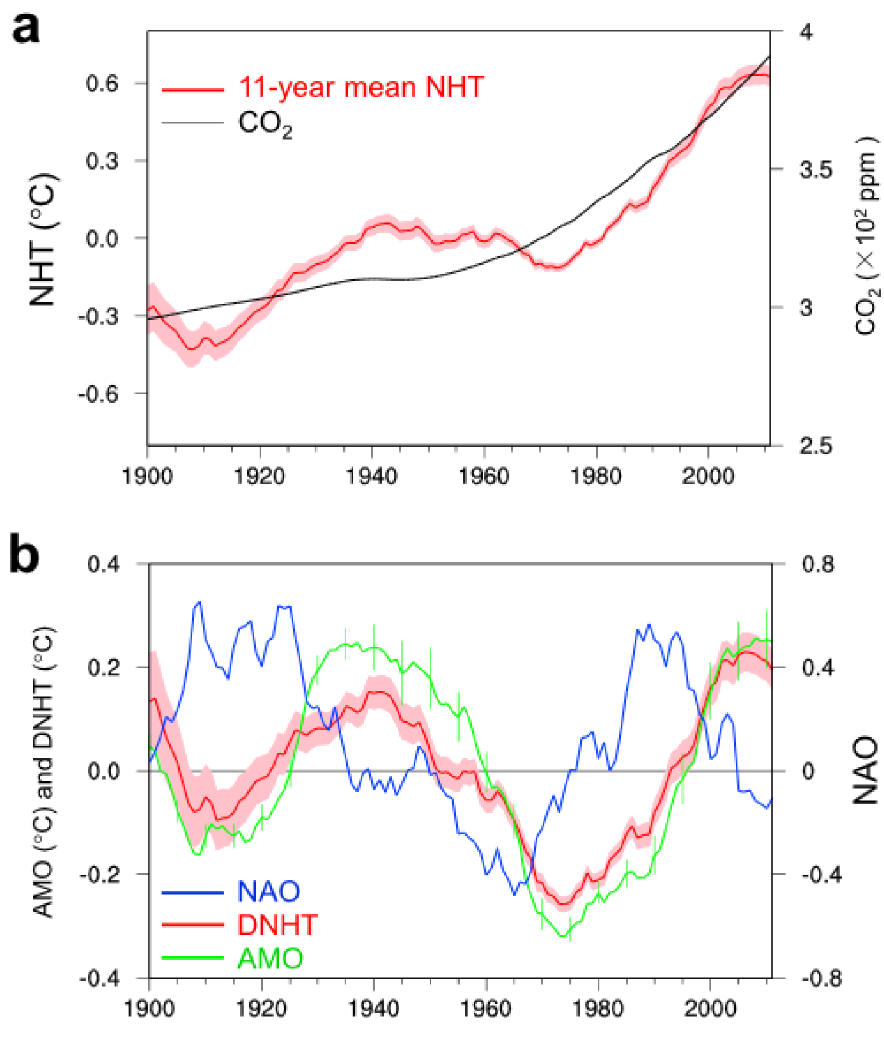

Figure 6. Northern Hemisphere Temperature (NHT), North Atlantic Oscillation (NAO) and Atlantic Multi-decadal Oscillation (AMO) indexes from 1900 to 2011. (Source: Li & Jin (2013) [61]. Note: (**a**) The 11-year running mean (red line) NHT (averaged poleward of the equator) anomalies from the HadCRUT4 data set, relative to the base period 19611990. The black line shows the global atmospheric CO_2 concentrations. (**b**) The 11-year running means of DNHT (red), NAO (blue), and AMO (green) indices. The pink shaded areas in **Figure 1a,b** show the 2-sigma uncertainty ranges of the NHT series for the HadCRUT4 data set estimated using the 100 realizations. The vertical green line in **Figure 1b** shows the 2-sigma uncertainty ranges of the AMO series for the HadSST3 data set.

Christy and McNider also attempted to remove the global signal of multi-decadal oscillations such as the AMO and PDO from the post-1950 data in order to derive the residual rise, which they assumed would then reflect the climate sensitivity to rising GHGs, i.e., the transient response to global emissions [62]. Their transient climate sensitivity was 50% smaller than the average currently calculated by modelling studies. Thus, the multi-decadal cycles peaking in the post-1950 period may account for 0.4 °C of the late centennial rise in GSAT in the Northern Hemisphere (variously estimated at 0.8 °C). However, we should note that these authors did not address the underlying recovery from the LIA, though Christy and McNider (2017) [62] referred to its presence, and thus their estimates of Transient Climate Sensitivity need to be seen in this context.

Scafetta and colleagues have come to the same conclusion with regard to transient climate sensitivity derived from their harmonic model – that current estimates need to be halved toward a mean value of 1.5 °C (see Section 5).

4. Mechanisms

4.1. Cycles of Heat Storage and Release

The heat capacity of the oceans is three orders of magnitude higher than the atmosphere and the oceans are hence the only significant form of heat storage of solar energy, having sequestered over 80∼90% of heat generated by observed global warming [39]. Most of the heat stored from the input of solar energy remains initially within the upper 300 m of the surface layers of a stratified ocean. It is thereafter subjected to the main processes that redistribute heat in surface waters, such as ENSO and the surface currents of the global 'conveyor belt' which discharge large amounts of heat form the Gulf Stream in the Atlantic, the Kuroshio Current in the North Pacific and the circumpolar currents of the Southern Ocean. Localised zones of down-welling in the North Atlantic and North Pacific take heat to depths between 700∼2000 m, for example, in the Atlantic Meridional Overturning Circulation – AMOC. Zones of upwelling can also release heat to cooler surface waters off Antarctica and are thought to 'drive' the AMOC. Periodic upwelling of cold deep water off Peru drives the El Nino oscillation.

The main inter-hemispheric oceanic heat exchange – the AMOC, has oscillations on timescales of 1000 years, but the speed of the AMOC also shows multi-decadal oscillatory behaviour [51, 56–59]. The overturning circulation is the main candidate for a heat cycle on a millennial timescale and a recent slowdown has been reported, understood to have led to a cooling of North Atlantic surface waters, but also to storage of heat at depth in the South Atlantic and Southern Oceans [56–59]. However, the observational record is limited – a slowdown from 2005 to 2010 has stabilised, and the AMOC appears to be in a 30% reduced state [63–66].

4.2. The Phenomenon of 'Hiatus' in Global Warming

The rise in GSAT shows two distinct slowdowns – hiatus, when over several decades, GSAT remained essentially flat: 1945–1975 and 2000–2015 (**Figure 2**). Since GSAT is a reflection of ocean surface temperatures, a number of studies sought the 'missing heat' in the deeper ocean, and a thorough review concluded the middle waters of the Atlantic were the main heat sink [67]. An increased speed of the AMOC may cause heat sequestration at depth in the North Atlantic and the pause in GSAT coincides with the slow down noted since 2005 [64]. Further, the Southern Ocean zones of upwelling and down-welling involve multi-decadal patterns of heat storage and release that are also tele-connected globally [68, 69]. A similar 'hiatus' in GSAT, between 1945–1975, coincided with the negative phases of the main Pacific (IPO) and Atlantic (AMO) multi-decadal cycles, and conversely, the rises in GSAT between 1920–1945 and 1975–2000, coincide with the positive phases of these two cycles (**Figure 6**) [61, 70, 71].

4.3. Multi-Decadal Ocean Cycles and Predictive Models

Recent attempts have been made to incorporate specific ocean cycles into the coupled Global Circulation Models and have provided results on a decadal timescale: for the North Atlantic Oscillation – NAO [72]. Very recently, modellers led by the Max Planck Institute for Meteorology in Hamburg, have attempted a revised treatment of 'internal variability' across a full suite of CMIP models including those of the

Geophysical Fluid Dynamics Laboratory (GFDL) that was central to early modelling studies. The authors concluded that when ocean cycles are taken into account there may be no further global warming for several decades due to the operation of natural forces supressing the apparent anthropogenic global warming signal [6].

There remain acknowledged difficulties incorporating longer cycles into models due to: (a) irregular periods and amplitudes; (b) initialisation, i.e., when model runs are initiated the difficulty is knowing where to begin the cycle [73, 74]. Modellers thus revert to factoring in some form of generalised internal variability when dealing with low frequency oscillations, as we see from **Figure 1** (see discussion on evaluation of models by Flato et al. in the IPCC 5th report pp. 741–866 [75], and discussion in Section 5 with regard to semi-empirical harmonic models.

4.4. Multi-Decadal Shifts in Cloud Cover

It seems clear with regard to storage and release of heat, particularly with ENSO, that a relaxation oscillator [52] is at work, and the concept has been extended to longer term cycles [20, 22]. With regard to mechanism, in the case of ENSO, at least, during the cool Nina negative phases, clearer skies allow the oceans to absorb more solar energy, which is released in waves to the atmosphere during the Nino positive phase [69–71]. It can be expected that all of the shorter ocean cycles involve surface waters to a depth of perhaps 300 m. Whether there are similar cycles of cloudiness and clear sky (to ENSO) has not been established - though during the critical global warming period 1983–2001, satellite surveillance under the International Satellite Cloud Climatology Project (ISCCP) showed a steady drop of 4% in reflective low-level cloud cover over the oceans [44–46, 76]. This data set was criticised as subject to satellite calibration error [4]: chapter 7, p. 208. and as conflicting with some ocean surface-based assessments [76]. However, extensive work has continued, and a new data set is available confirming the critical 1983–2001 period of decline in global cloud cover [45].

Extensive research on correlations and mechanisms with regard to cloud cover has been ongoing at CERN, Geneva [16]. The latest reports suggest the cloud-seeding effect expected during cycles of low solar magnetic activity and consequent high cosmic ray flux (e.g., during the LIA) is not likely to prove significant [77]. The effect of UV-flux and stratospheric to tropospheric influences remains a key area of study (see below).

However, trends in short-wave radiation flux to the land surface over this period have been ascribed to shifts in cloud cover with some confidence. For example, the Short Wave radiation flux increased at 0.87 W/m²/decade from 1982–2008 [78], and this wattage input at the surface can be compared to the recent spectrally resolved radiation studies of CO_2 rising at 0.2 W/m²/decade measured between 2001 and 2010 [40]. The same measurement team report a parallel rise of 2 W/m^2 of Infra-Red radiation from clouds and water vapour over the same period. This data confirms the powerful effect of oceanic sources of cloud and water vapour, as described by Compo and Sardeshmukh [14]. Land surface temperatures are thus strongly dependent upon wind direction, a factor seen clearly in Southern Ocean studies and Antarctic temperatures [34], as well as sudden warming events in Greenland [17].

It has been argued that cloud thinning and the increase in insolation could be a feedback to surface warming trends attributed to rising CO_2 levels [79]. However, cloud thinning appears to have stabilised after 2001 in tandem with the hiatus in GSAT (until the 2016 ENSO event) despite the cumulative impact of CO_2 emissions.

On a regional level, clouds have been shown to play a major role in the complex Arctic Oscillation [80]. Given that the Arctic is a zone of net heat loss, the presence of clouds acts as a conservation force, warming the surface and reducing heat loss from the ocean. Over the period 1980–2004, cloud cover over the Arctic Ocean increased by 14% [80, 81]: and see: https://www.pmel.noaa.gov/arctic-zone/detect/climate-clouds.shtml. In this period, not only did atmospheric circulation change, but ocean currents brought more warm water into the Norwegian Sea and Barents Sea. Floating sea-ice cover fell by 50% in summer and 10% in winter, thus increasing the flow of heat and moisture to the atmosphere [80, 81].

There is no comparable data for the Arctic prior to the satellite era, but temperature patterns over the longer period show an assumed natural warming peak in the late 1930s and early 1940s [54, 55]. The amplitude from the recent trough of the AO (roughly 1970) to its current peak (2010–2019) is 3 °C on average for all the circumpolar stations (https://arctic.noaa.gov/Portals/7/ArcticReportCard/Documents/ArcticReportCard_full_report2019.pdf), and compares with 2 °C expected from the natural cycle peaking again. Furthermore, the rate of change of the previous and presumed natural warming from 1920–1945, is the same as the rate from 1980–2000 despite the latter being generally regarded as forced by anthropogenic greenhouse gases.

Changes in the Arctic have implications for the Northern Hemisphere: the dynamics and teleconnections of the variable polar vortex have an effect upon storm tracks in this NE Atlantic region and show a wider hemispheric impact [82]. For example, recent analysis of glacial dynamics and proxies for winter precipitation in Norway show a correlation to a strong polar vortex - wetter, as in the recent warm period, and drier, as in the LIA, with clear oscillatory behaviour through the Holocene [80–85].

These recent studies of cloud behaviour, storm tracts, the polar vortex and teleconnections add weight to the proposition that clouds – in percentage global cover, and spatial distribution, may prove to be the proximal source of ocean heating and cooling cycles. Cloud cover north of 45° acts as an insulating and hence warming force, and southward of that, a cooling force – thus dispositional changes as well as overall percentage change may result from shifts in the Jetstream track, which may be linked to changes in solar-UV activity and cycles of magnetic variability [46, 82, 85].

Recent analysis from the CERES satellite programme [43, 86] examines 2.4 decades of observations of Absorbed Solar Radiation (ASR) and Outgoing Long Wave Radiation (OLR) in relation to Earth Energy Imbalance (EEI) calculations. The data confirm the long-standing approximately 0.4 W/m^{-2} value for the EEI, thus demonstrating that the earth's system is gaining heat, however these studies conclude that the dominant source of the imbalance is ASR which increased substantially from 2000∼2024 at 0.797 Wm^2/decade. The ASR tracks the rise in Sea Surface Temperatures – with no significant trend in surface temperatures from 2000∼2015 and then a strong rise due to the 2016 major El Nino event (**Figure 7**). These studies flag 'cloud changes' as the source of the increase in incoming Short Wave radiation at the surface. These figures can be compared to the rate of increase of CO_2 radiation at the surface (0.2 Wm^{-2}/decade, or 0.44 Watts over the 2.4 decade time period) and the tracking of SSTs during this period points to ASR being the main driver: 0.44/1.91 = 23% is left for the CO_2 driving force.

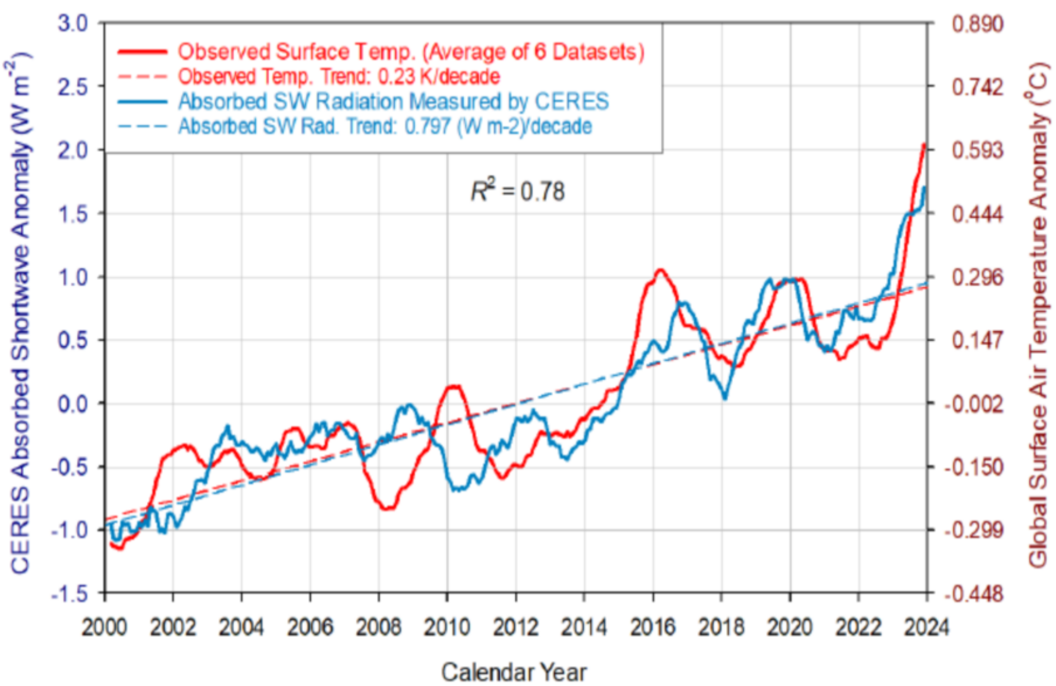

Figure 7. The relation of Absorbed Solar Radiation to Surface Temperature from 2000∼2024. Source: Nikolev & Zeller, 2024 [43]: Figure 7.

We are therefore left with a major question to resolve. There is evidence that the absorption of Short Wave radiation at the surface during the critical 1980∼2000 and 2015∼2024 warming periods dominates over the CO_2 radiative forcing. This cloud-thinning could be a feedback from rising ocean temperatures, or it could be a cause. Ultimately, all warming of the ocean is due to absorbed solar radiation, and there are well-attested natural cycles of warming and cooling. Furthermore, rates of change during the main period of rising CO_2 concentrations do not differ substantially from rates of change prior to those emissions. The question therefore arises as to whether the (largely) modelled effect of rising CO_2 has been over-estimated.

4.5. External Factors of Causation

Although ocean oscillations may be regarded as internal to the earth-system, there remains the potential for an external 'excitation' of the oscillator, such as cycles of solar activity as originally proposed by Bond et al.[26]. Various attempts at calculating solar influence have largely focussed upon variability of visible wavelengths and IPCC has concluded that solar changes are too small in effect compared to GHG forcing estimates[87]: chapter 2.1; and discussion by Myhre et al., p. 689]. The focus on visible wavelengths may be misplaced. The polar vortex is affected by variations in solar-UV flux, with periods of high solar activity correlating to poleward shifts of the sub-tropical jets and increased westerlies[82, 85, 88]. Furthermore, the millennial sediment (Bond) cycle in the North Atlantic showed correlations to changes in dust deposition on the Greenland icecap - a proxy for changes in wind direction, which in itself is a proxy for a contracted polar vortex[26]. Increasing solar activity since 1600 CE[16] would be expected to increase the strength of the polar vortex and transfer of heat poleward.

In the context of a variable polar vortex, Christiansen demonstrated the existence of two North Atlantic circulation regimes corresponding to weak and strong polar vortices, with a regime shift in the mid-1970s coincident with the later global warming period identified here[88]. The LIA itself correlates with low solar activity (and hence low UV flux) and a period of shifts in oceanic wind direction cycles[88, 89]. Further, correlation of dust proxies with centennial oscillations of the Antarctic Circumpolar Current points to changes in wind regime in the Southern Ocean, with a potential to drive global cycles[34].

There is thus a developing hypothesis relating to far-UV flux (part of Total Solar Irradiation – TSI), discussed briefly by the IPCC[86]: WG1, chapter 2, pp. 192–193, whereby the UV-flux influences the polar vortex, cloud cover and wind patterns. The UV flux, though weak in wattage at the TOA, has a greater amplitude (26%) over the LIA cycle than the visible wavelength (0.4%) but IPCC has concluded there is very low understanding of the science and does not take the issue further[4]: discussion by Myhre et al., p. 690. However, a wavelet analysis on the Total Solar Irradiation – TSI, from a reconstruction based on cosmogenic isotopes by Stuiver and Brazunias in 1993, is reviewed in the IPCC 5th WG1 report ([4], p. 390) and a significant peak at 980 years is evident – matching the correlation noted by Bond et al., in 2001[16] and recently, Scafetta and Bianchini also identify through harmonic analysis a 980-year cycle in solar activity parallel to paleo-climate cycles of the same period, implying a solar driver[89, 90].

With the proviso that UV variability and effects upon the Jetstream, storm tracks, clouds and potential regime shifts may be significant but remain unquantified, it is therefore concluded that centennial and millennial scale cycles are likely caused by a combination of internal oscillatory mechanisms potentially modified or excited by documented cycles of solar activity[88–92].

4.6. Recent 'Extreme Weather', Polar Warming and a 'Wavy' Jetstream

In the last decade, extreme weather events such as heatwaves, wildfires, floods, drought and a descending polar vortex leading to extreme cold events, particularly in the Northern Hemisphere, correlate to a shift in Jetstream track. It has been proposed that anthropogenic warming and polar amplification of that warming (mediated by loss of Arctic summer sea-ice) may have caused an observed shift to a 'wavier' Jetstream[82, 83, 85, 93–96]. However, the connection to polar amplification has been questioned as the trends are not consistent[96].

These studies follow the orthodoxy of attribution studies without reference to longer-term cyclic behaviour. However, it may well be that the current Arctic warming exceeds that of previous cycles and that a sea-ice threshold has been crossed with significant impact on Northern Hemisphere weather patterns. We should note that during the Holocene Temperature Optimum, the Arctic Ocean was ice-free[97], and that a global regime shift that desiccated the Sahara (5-3 Kyr BP) followed this temperature optimum[83]. These changes followed a decline in insolation in the northern hemisphere caused by the orbital precession cycle. (see: https://www.nature.com/scitable/knowledge/library/green-sahara-african-humid-periods-paced-by-82884405/).

Whatever the attribution, a long-term oscillation model has been proposed that invokes changes in wind strength, which then correlate with warming and cooling phases in the ice-core record[20, 22, 34]. Wind strength is related to the pole-to-equator difference and during warming this lessens as more heat is transferred to polar regions and the greater the differential, the stronger the Jetstream, and vice-versa. A weaker Jetstream tends to be wavier – this happens during the polar summers, but a more sustained waviness may be expected to cool the global surface. In terms of planetary thermo-dynamics, a meridional down-loop will send cold Arctic air toward the equator, hence cooling warm regions, and on the up-loop, warm sub-tropical air is displaced to regions of permanent heat-loss, also leading then to net cooling. In the oscillatory model warming-leads-to-cooling-leads-to-warming[34]. Thus, current observations of a wavier Jetstream may or may not be the first sign of a cooling feedback from global warming[92–96].

5. Predictions for the 21st Century

The issue with future predictions is the question of *cycles*. There is evidence from ocean heating cycles of a waveform that may be peaking in the early 21st century. The wave would then decline at first due to multi-decadal variability such as the 60-year global oscillation, and then over a series of such cycles, rising and falling as part of the descending curve of the millennial cycle of which the LIA was the last cold period[11, 35]. Similar extrapolations can be made from the ice-core data[34] (see **Figure 4**). Potential future declines in the solar cycle as occurred during the LIA may also come into play. There are also uncertainties with regard to effective radiative forcing of anthropogenic greenhouse gases and the level of future emissions (see below).

There are three potential approaches to 21st century prediction with respect to cycles: 1) to extrapolate the natural wave-form of cycles of known periodicity; 2) to incorporate internal ocean oscillations into GCM models; 3) to incorporate solar cycle changes of activity into GCM radiation fluxes – in particular the effects of far-UV. Here we briefly review examples of these three approaches.

However, it is important to note that there is a key issue with the standard suite of CMIP predictive models other than the poorly resolved cycles which receive wide discussion in circles outside of the IPCC consensus but are not reflected within the latest report, and that is how chaotic factors may confound the model predictions. Edward Lorenz, widely regarded as the founding father of computerised weather prediction, warned that very small uncertainties (or errors) would be amplified during iteration of computer runs[98]. He warned particularly that iterative runs in predictive models were unsuitable for problems where progressive changes from one regime of behaviour to another play a role. This may be the case with regard to cyclic behaviour – for example, long-term variability of the AMOC and millennial shifts in wind regimes (see **Figure 4**).

There is very recent analysis of such factors as presented in one of the foremost climate models by a coding specialist[99]. Willis Eschenbach describes how clear errors are identified by the modellers as-and-when the initial model run predicts impossible results and these are corrected by scientifically unsupported fudge-factors to prevent the iterations repeating and magnifying the error.

5.1. Extrapolation of Wave-Forms

With regard to extrapolation of waveforms, cycles of approximately 100, 200, and 1100 years have been found in spectrographic analyses of 2500 years of tree-ring data on the Tibetan Plateau. Temperatures on the Plateau tend to reflect the global temperature[19]. Liu and colleagues projected the sine wave pattern of centennial and millennial wave-forms to predict a downturn (under natural conditions) on the Plateau by 2068. It would therefore be possible to determine the expected effect of the long cycle on GSAT by comparison of past correlations with the plateau. The peak to trough amplitude of the last millennial cycle on the plateau is about 0.8 °C and close to the amplitude of the global cycle. The predicted fall to 2068, largely driven by the centennial wave form, is about half that amplitude and is followed by a rise and fall pattern into the next trough in the millennial cycle—i.e., an LIA (in about 400 years). An expected decadal rate of (natural) decline to 2068—i.e., 0.4 °C/6, would therefore be 0.06 °C/decade. This compares to the current (last 50-year) global warming signal of 0.14 °C/decade (see **Figure 1**), and the long-term rate of change over the past 12 decades at 0.08 °C/decade. Thus, if the 20th century rise is 100% anthropogenic, this will counter any cooling trend and warming will continue in the face of a declining natural cycle. On the other hand, if as here suspected, the figure is 50% or higher for natural forces, at 0.07∼0.09 °C/decade, then a slight cooling of 0.01 °C/decade will ensue.

The extrapolation of waveforms derived from both environmental data and parallel correlated waveforms from solar-activity cycles has been extensively explored by Scafetta[100–103], and recently reviewed by a large inter-disciplinary group – Connolly et al., which also looked at models of solar irradiance[104]. Scaffeta and colleagues concluded that over 60% of the post-industrial warming can be explained by harmonic interactions of known cycles derived from spectral analysis of temperature data sets, and by extrapolating these cycles in a semi-empirical harmonic model came to the conclusion that the next few decades would be affected by a cooling phase of natural forcing. This work also implies that CMIP models and extrapolations are in error by a factor of two.

The Connolly review group draws attention to the IPCC selective use of analyses of past solar activity, where studies that conclude minimal centennial change in solar flux are preferred, whilst downplaying as outliers otherwise competent analyses that would accord solar output a significant proportion of the global warming signal. The group (23 experts in this field) concluded: 'It appears that the CMIP6 modelling groups have been actively encouraged to consider only one estimate of TSI for the 1850- present period. In terms of scientific objectivity, this seems to us to have been an approach that is not compatible with the results already published in the scientific literature and even unwise relative to the results highlighted by this paper and of other recently published works' ([104], p. 56).

Similarly, wave-forms in the Antarctic temperature proxies (see **Figure 4**) can be extrapolated to show an expected (natural) cooling phase with multi-decadal steps toward the next LIA in 300 years[34]. Of course, these natural forces will compete with the expected rising levels of anthropogenic GHGs. Ironically, considering the efforts at mitigation, natural cycles may now be leading to the next glacial cycle and GHG levels would have a potential meliorating effect.

5.2. Incorporating Internal Ocean Oscillations into GCM Models

Incorporating low-frequency cycles into models encounters many difficulties, and as we have seen from references in the IPCC's 6th report, the current orthodoxy is to presume a small amplitude for low frequency variability together with the 'cancelling out' of shorter frequency cycles in the longer term. However, as we saw in Section 3, some models that incorporate ocean cycles predict either decadal scale flat-lining or some cooling[6, 63].

5.3. Incorporating Solar Cycle Changes of Activity into GCM Radiation Fluxes

As outlined, there are correlations of the millennial cycle with solar activity. During the first part of the 21st century solar output declined in the preferred IPCC analyses, but not so much in others[101]. The consensus position is that the current run of low peaks in the Schwabe cycle will produce a 'Dalton' type minimum of 2∼3 low peaks[102–104], but some specialists argue that there could be a prolonged minimum as occurred during the LIA[105].

With this potential solar decline in mind, two computer studies, one at the US National Centre for Atmospheric Research[29] and the other at the Hadley Centre in the UK[30], have attempted to model the competing effects of increasing greenhouse gases and an assumed decline in solar activity associated with a recurrent Maunder Minimum as occurred in the LIA.

The Hadley research used standard (for 2012) conversion factors for the effects of CO_2, together with a relatively small adjustment regarding solar parameters in their model; whereas the NCAR study attempts to factor-in changes in UV flux with effects upon the Jetstream, a larger amplitude for the LIA solar factor (i.e., in the prospective decline). There are also revised factors for conversion of radiation fluxes from CO_2 to surface temperature[41]. In the Hadley study, the world continues to warm but at a lesser rate to 2060, thereafter increasing; in the NCAR study, there is a cooling to 2030 and a moderate recovery after 2060.

There is some expectation therefore that the current warm period will peak in the current decade (2020s), and that centennial and decadal cycles will create a short decline thereafter. According to the long-wave (with recent period of about 1000 years), there may be a plateau with some higher peaks and a new trough or LIA may well be 300–400 years hence.

However, continual emission of anthropogenic greenhouse gases will compete with the driving forces of natural change, and how much the rise in the main component - carbon dioxide, can be expected to ameliorate a possible decline in solar output, depends upon the accuracy of radiative forcing (RF) assessments as well as their conversion to surface temperature change. as well as any cloud and consequent insolation changes. One study at the Hemholz Fluid Dynamics Laboratory in Dresden utilised regression analysis of the solar aa index with temperature and carbon dioxide concentrations to predict future temperatures, finding first an indication that climate sensitivity to CO_2 was low (between 0.6∼1.4 K) and that there is a potential for cooling in the 21st century related to extrapolation of solar magnetic activity [107].

One conclusion from this assessment of predictions is that the majority of the current (CMIP6) suite of models may have over-estimated the Radiative Forcing conversion factor for surface temperature by a factor of two.

Ironically, on a longer timescale, higher levels of CO_2, if accorded the power assumed by the models, could help to ameliorate a longer-term scheduled descent into the next Ice Age. However, a recent study of CO_2 cycles over millions of years finds that above 400 ppmv sea-surface microlayer acidification is correlated to oceanic mass extinction event. Thus, although CO_2 emissions may not be the main driver of changes in temperature, they need to be radically reduced to avert ocean anoxia events that would threaten all life on the planet [108].

6. Conclusions and Implications for Policy and Research

The evidence of paleo-climate studies points to a relatively small impact of anthropogenic activity during pre-industrial times and to a natural millennial cycle rising from a trough in a regular pre-industrial cycle to the present day, contributing to a modern warm period in line with the peaking of the millennial cycle. The view that most of the *centennial* warming is anthropogenic arises from a misreading of the IPCC consensus position. In fact, IPCC attribute most of the pre-1950 centennial warming to 'natural variability', i.e., for the period when the CO_2 effect was marginal. Since 1950, IPCC statements assert 'most' of the post-1979 warming is anthropogenic but do not provide a more accurate percentage figure. Most' is regarded as greater than 60%, but this is also a judgement made by selected professionals and there are estimates of 50% natural component in the literature—e.g. Scafetta [103]. Thus a 70–75% natural component of the centennial warming since pre-industrial times cannot be ruled out. Early models did not incorporate oceanographic cycles of heat storage, and just as the up-phase will have contributed to past warming, there is a clear potential for the down-phase of cycles to counter future warming.

Estimates of the percentage contribution of natural vs anthropogenic causes can be drawn from paleoclimate data and modern surface measurements of radiation flux such that a 60∼75% figure can be derived for the natural driver.

This conclusion is supported by consideration of marginal radiative forcing changes due to anthropogenic greenhouse gases compared to variability of cloud cover and insolation at the surface of the Earth, particularly during the post-1950 global warming period. Questions of cause and effect remain, particularly regarding natural shifts in cloud cover.

The mechanisms of cyclic heat storage and release are poorly constrained, but recent analyses point to a combination of changes in solar activity in the far-UV spectrum, effects upon the polar vortex, and changes in wind strength and direction affecting cloud cover and water vapour content. Modelling has begun to incorporate both oceanographic oscillations as well as consideration of a future decline in solar activity and effects upon the polar vortex – with studies showing the potential for no further warming for several decades and even the possibility of cooling (even as a consequence of past warming). No further natural warming until after mid-century is also in-line with projections based on spectral analysis of past cycles.

With regard to research directions, further analysis of solar magnetic cycles and UV-flux may reveal correlations with variable Jetstream dynamics and the disposition of cloud cover, which may be highly relevant to warming and cooling cycles. For example, percentage changes in *zonal* winds are correlated with high solar activity and fast Jetstream. Whereas *meridional* winds are correlated with low solar activity and slowing Jetstream, and may potentially alter heat storage in the oceans, the extent of polar sea-ice, freshwater input to the Arctic Ocean, and the speed of the global Thermo-Haline Circulation or Ocean Conveyor Belt, thus affecting the global heat balance (see NOAA: https://oceanservice.noaa.gov/facts/conveyor.html).

Given the media focus upon ever-rising temperatures, the relevance for policy of the above conclusions with regard to a future lack of surface warming is profound. The phenomenon of 'prior commitment' and faith in models must be balanced by appropriate analysis of real-world data—as happened in relation to ocean pollution under policies of 'dilute and disperse' [83, 109]. Such analysis would need to be followed by admission that models have serious limitations for setting policy and that in a less certain world, policies that promote resilience to change in either direction demand greater attention. If human emissions contribute as little as 25% to the observed warming, halving those emissions at great cost will address only 12.5% of the driving force and have only marginal effect upon how the climate changes.

Thus, this percentage issue becomes an important factor in the technical feasibility and cost not just of renewable energy sources, or sunlight manipulation but also the 'capture' of carbon from flue-gas discharge or from installations that suck the gas from the ambient air. There is a growing sense of urgency with regard to emission reduction and technologies for capturing and sequestrating carbon. The UK government, for example, has announced the ARIA programme for tenders related to research in these fields [110], and has budgeted £22 billion over 10 years for capturing carbon from off-gases (from gas-fired power stations) and burying it in exhausted UK gas-fields – this from an economy that is struggling to maintain social services. Competing costs will be a key issue in future policy options.

On the other hand, it would be prudent to mitigate the future increase of emissions in the light of the recent analysis of extinction threat due to ocean acidification [108]. There is an urgent need to explore costs, timescales and marine dynamics on this issue. In addition to the technological choices regarding renewable energy, there is a potential for the sequestration or removal of carbon dioxide form the air [111] if it could be could be extensive enough and economical.

Funding

This review received no funding apart from crowd funding among friends to cover conference expenses (Prague, 2019) and publication fees.

Institutional Review Board Statement

Not applicable.

Informed Consent Statement

Not applicable.

Data Availability Statement

Data sources are given in the text.

Acknowledgements

This paper arose from an invited keynote presentation at the Prague 2019 3rd World Summit on Global Warming and Climate Change Science. I thank Gilbert Compo and Prashant Sardeshmukh for conversations at Colorado University on ocean heat transfer; and Professor Venkatachalam Ramaswamy at the Prague conference for discussion on model limitations with regard to cycles. I am indebted to Professor Jackson Davis at ESI for reading the manuscript, for his detailed and inspirational analysis of Antarctic ice-core data, and for Modtrans calculations to support the presentation of data of Radiative Forcing and historic carbon dioxide levels. I thank Dr Elena Koslova at Exeter University for identifying the important Buentgen et al. critique and for reading the manuscript.

Conflict of Interest

The author declares no conflicts of interest.

Abbreviation

ACO	Antarctic Centennial Oscillation
AGW	Anthropogenic Global Warming
AIM	Antarctic Isotope Maxima
AMO	Atlantic Multi-decadal Oscillation
AMOC	Atlantic Meridional Overturning Circulation
AO	Arctic Oscillation
ASR	Absorbed Solar Radiation
BP	Before Present
CE	Common Era
CERN	European Organisation for Nuclear Research
CLINTEL	Climate Intelligence (Group)
CMIP	Community Model Inter-comparison Project
D/O	Dansgaard/Oeschger (cycles)
DNHT	De-trended Northern Hemisphere Temperature
ENSO	El Nino Southern Oscillation
GCM	General Circulation Models
GFDL	Geophysical Fluid Dynamics Laboratory (Princeton, USA)
GHG	Greenhouse Gases
GSAT	Global Surface Atmospheric Temperature
GMST	Global Mean Surface Temperature
IPCC	Inter-governmental Panel on Climate Change
IPO	Inter-decadal Pacific Oscillation
ISCCP	International Cloud Climatology Project
LIA	Little Ice Age
MWP	Medieval Warm Period
NAM	Northern Annular Mode
NAO	North Atlantic Oscillation
NCAR	national centre for Atmospheric Research (USA)
NH	Northern Hemisphere
NHT	Northern Hemisphere Temperature
OHC	Ocean Heat Content
OLR	Outgoing Long wave Radiation
PDO	Pacific Decadal Oscillation
RF	Radiative Forcing
SAM	Southern Annular Mode
SPM	Summary for Policy Makers (of IPCC Working Group Reports)
THC	Thermo-Haline Circulation
TOA	Top of Atmosphere
TSI	Total Solar Irradiation
WG1	Working Group 1 (of IPCC)

Appendix A

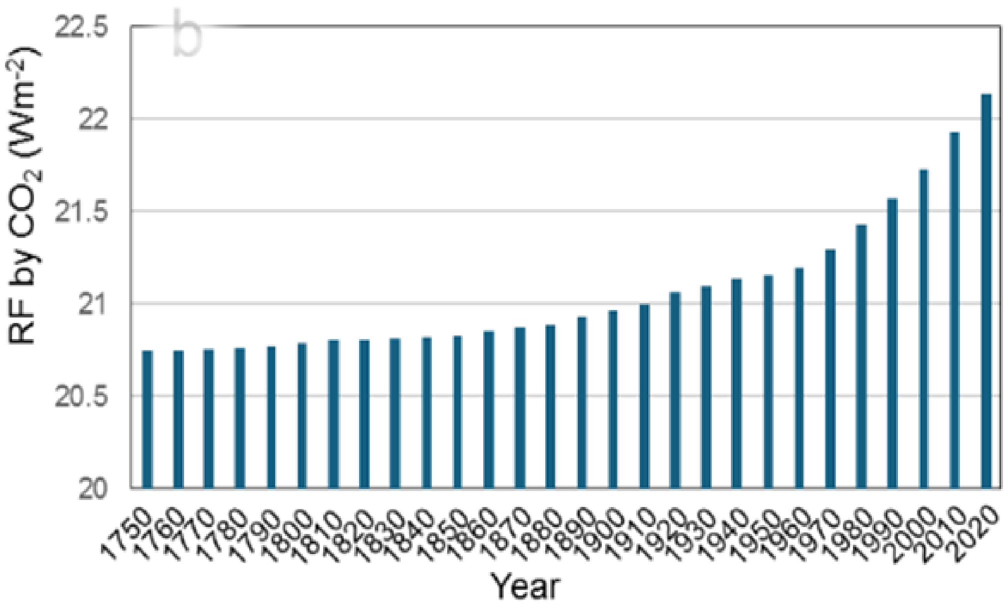

(**a**)

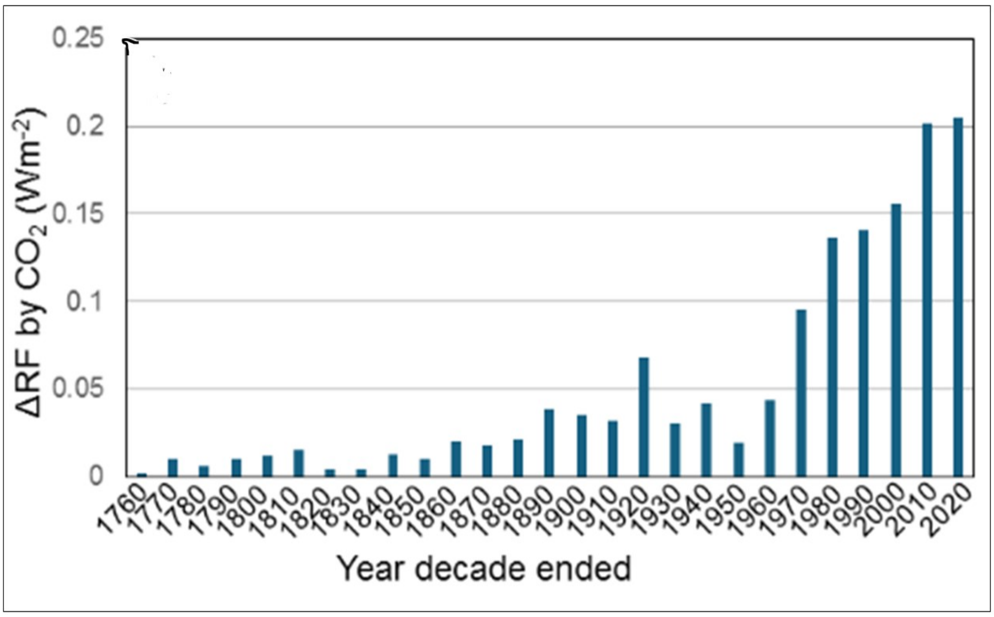

(**b**)

Figure A1. Radiative forcing (RF) at the top of the atmosphere from atmospheric carbon dioxide (CO_2) by decade, 1750–2020 (**a**) and corresponding marginal change in forcing by decade (**b**), computed using the atmospheric absorption/transmittance code MODTRAN. Original data on atmospheric CO_2 concentration are from the National Ocean and Atmospheric Administration (NOAA) and the Eidgenössische Technische Hochschule Zürich (ETHZ) as reported in Our World in Data and the Global Carbon Project. From https://www.climate.gov/media/14596 (retrieved November 28, 2024). See **Figure A2**, below.

Original measurements on CO_2 concentration were made from the graphical display twice using a blinded protocol. The re-measurement error (mean of the difference between the first and second measurements) was 0.0651% (second blind measurement minus the first divided by the second × 100). See **Table A1**.

Radiative forcing was computed using the mid-latitude forcing curve in Figure 8a of W. J. Davis (2017, Figure 8a)[112] corresponding to a clear sky, for which the best fit (R2 = 0.9918) logarithmic function is y = 3.4221ln(x) + 1.4926. Graphs and underlying analysis provided by W. J. Davis (personal communication).

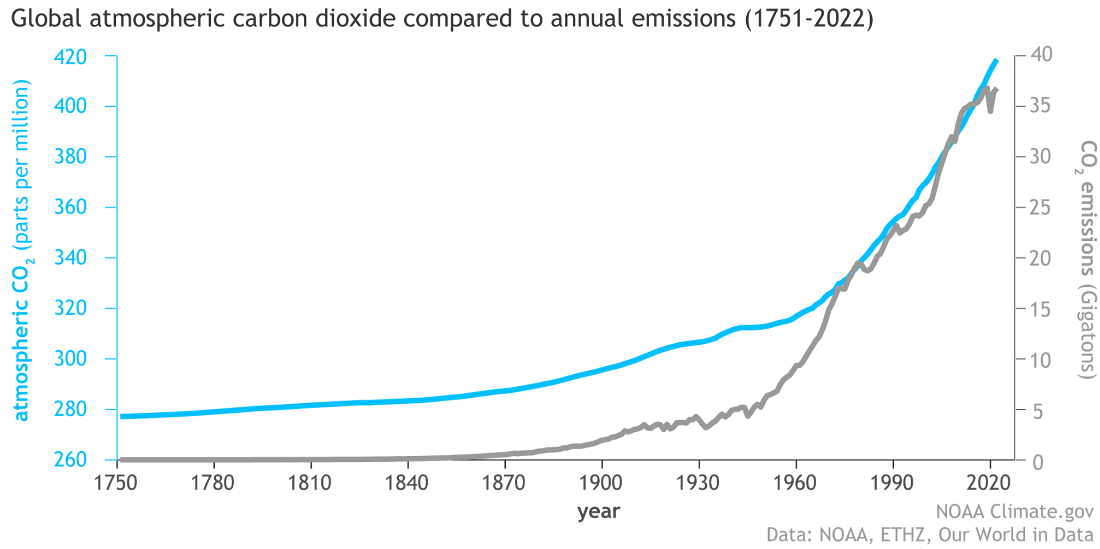

Figure A2. Global atmospheric carbon dioxide atmospheric levels from pre-industrial times (1750) to 2022 (blue line) and industrial emissions (grey line).

Table A1. Radiative forcing (RF) at the top of the atmosphere from atmospheric carbon dioxide (CO_2) by decade, 1750–2020, and corresponding change in forcing by decade, computed using the atmospheric absorption/transmittance code MODTRAN.

Year	First Measurement (ppmv)	Second (Blind) Measurement	Percent Difference	Mean ppmv	CO_2 Forcing	Decadal Forcing Increase
1750	277.5	278	0.18	277.75	20.7478	
1760	277.7	278.1	0.14	277.90	20.7497	0.00184
1770	278.5	279	0.18	278.75	20.7601	0.01045
1780	279	279.5	0.18	279.25	20.7662	0.00613
1790	280.1	280	−0.04	280.05	20.7760	0.00979
1800	281	281	0.00	281.00	20.7876	0.01158
1810	283	281.5	−0.53	282.25	20.8028	0.01518
1820	283.2	282	−0.43	282.60	20.8070	0.00424
1830	283.4	282.5	−0.32	282.95	20.8113	0.00423
1840	284	284	0.00	284.00	20.8240	0.01267
1850	284.5	285.2	0.25	284.85	20.8342	0.01022
1860	286	287	0.35	286.50	20.8539	0.01976
1870	288	288	0.00	288.00	20.8718	0.01787
1880	289.5	290	0.17	289.75	20.8925	0.02073
1890	293	293	0.00	293.00	20.9307	0.03817
1900	296	296	0.00	296.00	20.9656	0.03486
1910	299	298.5	−0.17	298.75	20.9972	0.03164
1920	304	305.5	0.49	304.75	21.0653	0.06804
1930	306.9	308	0.36	307.45	21.0955	0.03018
1940	311	311.5	0.16	311.25	21.1375	0.04203
1950	313	313	0.00	313.00	21.1567	0.01918
1960	316.5	317.5	0.31	317.00	21.2001	0.04345
1970	326	326	0.00	326.00	21.2959	0.09580
1980	338.5	340	0.44	339.25	21.4323	0.13633
1990	354	353	−0.28	353.50	21.5731	0.14080
2000	370	370	0.00	370.00	21.7292	0.15611
2010	392	393	0.25	392.50	21.9312	0.20201
2020	416.5	417	0.12	416.75	22.1364	0.20515

References

[1] Koutsoyiannis, D., 2020. Revisiting the global hydrological cycle: is it intensifying? Hydrology and Earth System Science. 24, 3899–3932. DOI: https://doi.org/10.5194/hess-24-3899-2020

[2] Ramaswamy, V., 2019. Presentation of IPCC Global Warming Projections. In Proceedings of the 3rd World Summit on Global Warming and Climate Change Science; Prague, Czech Republic, 27–28 February 2019. Available from: https://climate.euroscicon.com

[3] IPCC, 2021. Summary for Policymakers. In: Climate Change 2021: The Physical Science Basis. Contribution of Working Group I to the Sixth Assessment Report of the Intergovernmental Panel on Climate Change. Edited by Masson-Delmotte V., Zhai, P., Pirani, A., et al. pp. 3−32. Available from: https://www.ipcc.ch/report/ar6/wg1/downloads/report/IPCC_AR6_WGI_SPM.pdf

[4] IPCC, 2013. Fifth Assessment Report: Summary for Policy Makers: p5, Figure spm.3. Available from: https://ar5-syr.ipcc.ch/topic_summary.php

[5] IPCC, 2007. Intergovernmental Panel on Climate Change (IPCC). Climate Change 2007: The Physical Science Basis; Contribution of Working Group I to the Fourth Assessment Report of the Intergovernmental Panel on Climate Change; Edited by Solomon, S.; WG1, chapter 9, figure 9.5. Cambridge University Press: New York, NY, USA, 2007.

[6] Maher, N., Lehner, F., Marotzke, J., 2020. Quantifying the role of internal variability in the temperature we expect to observe in the coming decades. Environmental Research Letters. 15, 054014. DOI: https://doi.org/10.1088/1748-9326/ab7d02

[7] Satellite Lower Troposphere Temperature record, available from: https://www.drroyspencer.com/ (cited 6 May 2021).

[8] He, Y., Wang, K., Zhou, C., et al., 2018. A revisit of global dimming and brightening based on the sunshine duration. Geophysical Research Letters. 45, 4281–4289. DOI: https://doi.org/10.1029/2018GL077424

[9] Wild, M., Liepert, B., 2010. The Earth radiation balance as driver of the global hydrological cycle. Environmental Research Letters. 5, 025203. DOI: https://doi.org/10.1088/1748-9326/5/2/025203

[10] Stanhill, G.; Achiman, O., Rosa, R., et al., 2014. The cause of solar dimming and brightening at the Earth's surface during the last half century: evidence from measurements of sunshine duration. Journal of Geophysical Research -Atmosphere. 119, 10902–10911. DOI: https://doi.org/10.1002/2013JD021308

[11] Gebbie, G., 2019. Atlantic warming since the Little Ice Age. Oceanography. 32(1), 220–230. DOI: https://doi.org/10.5670/oceanog.2019.151

[12] Gebbie, G., Huybers, P., 2019. The Little Ice Age and 20th-century deep Pacific cooling, Science. 363, 70–74. Available from: https://www.whoi.edu/cms/files/Gebbie_Huybers2019_283624.pdf

[13] Giese, B.S., Seidel, H.F., Compo, G.P., et al., 2016. An ensemble of ocean reanalyses for 1815–2013 with sparse observational input. Journal of Geophysical Research - Oceans. 121, 6891–6910. DOI: https://doi.org/10.1002/2016JC012079

[14] Compo, G.P., Sardeshmukh, P.D., 2009. Oceanic influences on recent continental warming. Climate Dynamics. 32, 333–342. DOI: https://doi.org/10.1007/s00382-008-0448-9

[15] Compo, G.P., Sardesmukh, P.D., Whitaker, J.S., et al., 2013. Independent confirmation of global land warming without the use of station temperatures. Geophysical Research Letters. 40, 3170–3174. DOI: https://doi.org/10.1002/grl.50425

[16] Kirkby, J., 2007. Cosmic rays and climate. Surveys in Geophysics. 28, 333–375. DOI: https://doi.org/10.1007/s10712-008-9030-6

[17] Bond, G., Showers, W., Cheseby, M., et al., 1997. A pervasive millennial scale cycle in the North Atlantic Holocene and glacial climates. Science. 278, 1257. Available from: https://www.researchgate.net/profile/Irka_Hajdas/publication/200032725_A_pervasive_millennial-scale_cycle_in_the_North_Atlantic_Holocene_and_glacial_climates.pdf (cited 3 July 2020).

[18] Yiou, P., Fuhrer, K., Meeker, L.A., et al., 1997. Paleoclimatic variability inferred from the spectral analysis of Greenland and Antarctic ice-core data. Journal of Geophysical Research. 102(C12), 26441–26454. Available from: https://agupubs.onlinelibrary.wiley.com/doi/epdf/10.1029/97JC00158

[19] Liu, Y., Cai, Q.F., Song, H.M., et al., 2011. Amplitudes, rates, periodicities and causes of temperature variations in the past 2485 years and future trends over the central-eastern Tibetan Plateau. Chinese Science Bulletin. 56, 2986–2994. DOI: https://doi.org/10.1007/s11434-011-4713

[20] Davis, W.J., Taylor, P.J., Davis, W.B., 2018. The Antarctic Centennial Oscillation: A Natural Paleoclimate Cycle in the Southern Hemisphere That Influences Global Temperature. Climate. 6, 3. DOI: https://doi.org/10.3390/cli6010003

[21] Scafetta, N., 2021. Reconstruction of the Interannual to Millennial Scale Patterns of the Global Surface Temperature. Atmosphere. 12, 147. DOI: https://doi.org/10.3390/atmos12020147

[22] Davis, W.J., Taylor, P.J., Davis, W.B., 2019. The Origin and Propagation of the Antarctic Centennial Oscillation. Climate. 7(9), 112. DOI: https://doi.org/10.3390/cli7090112

[23] Schlesinger, M.E., 1994. An oscillation in the

global climate system of period 65-70 years. Nature. 367(6465), 723–726.

[24] Mazzarella, A., Scafetta, N., 2012. Evidences for a quasi-60-year North Atlantic Oscillation since 1700 and its meaning for global climate change. Theoretical Applied Climatology. 107, 599–609. DOI: https://doi.org/10.1007/s00704-011-0499-4

[25] Yiou, P., Jouzel, J., Johnsen, S., et al., 1995. Rapid oscillations in Vostok and GRIP ice-cores. Geophysical Research Letter. 22(16), 2179–2182. Available from: https://agupubs.onlinelibrary.wiley.com/doi/abs/10.1029/95GL02014

[26] Bond, G., Kromer, B., Beer, J., et al., 2001. Persistent solar influences on North Atlantic climate during the Holocene. Science. 294, 5549. Available from: http://www.essc.psu.edu/essc_web/seminars/spring2006/Mar1/Bond%20et%20al%202001.pdf

[27] Latif, M., Martin, T., Reintges, A., et al., 2017. Southern Ocean Decadal Variability and Predictability Current Climate Change Reports. 3(3), 163–173. DOI: https://doi.org/10.1007/s40641-017-0068-8

[28] CMIP. Available from: https://climatedataguide.ucar.edu/climate-model-evaluation/cmip-climate-model-intercomparison-project-overview

[29] Meehl, G.A., Arblaster, J.M., Marsh, D.R., 2013. Could a future "Grand Solar Minimum" like the Maunder Minimum stop global warming? Geophysical Research Letters. 40, 1789–1793. DOI: https://doi.org/10.1002/grl.50361

[30] Jones, G.S.; Lockwood, M., Stott, P.A. What influence will future solar activity changes over the 21st century have on projected global near-surface temperature changes? Journal of Geophysical Research 2012 117, D05103. DOI: https://doi.org/10.1029/2011JD017013

[31] Obrochta, S.P., Miyahara, H., Yokoyama, Y., et al., 2012. A re-examination of the evidence for the North Atlantic '1500-year cycle' Quaternary Science Reviews. 55, 23–33. DOI: https://doi.org/10.1016/j.quascirev.2012.08.008

[32] Hsu, K.J., 1998. Sun, climate, hunger and mass migration. Science in China (Series D: Earth Sciences). 41(5), 449–472.

[33] Davis, J.C., Bohling, G.C., 2001. The search for patterns in ice-core temperature curves. In: Gerhard, Harrison and Hanson, editors, Geological perspectives of global climate change, (AAPG Studies in Geology 47). Chapter 11, pp. 213–229. Available from: http://archives.datapages.com/data/specpubs/study47/CH11/ch11.htm

[34] Davis, W.J., Davis, W.B., 2020. Antarctic Winds: Pacemaker of Global Warming and Global Cooling, and the collapse of Civilisations. Climate. 8, 130. DOI: https://doi.org/10.3390/d8110130

[35] Büntgen, U., Arseneault, D., Boucher, E., et al., 2022. Recognising bias in Common Era temperature reconstructions Dendrochronologia. 74, 125982. DOI: https://doi.org/10.1016/j.dendro.2022.125982

[36] Neukom, R., Steiger, N., Kaufman, D., et al., 2022. Inconsistent comparison of temperature reconstructions over the Common Era. Dendrochronologia. 74, 125965. DOI: https://doi.org/10.1016/j.dendro.2022.125965

[37] PAGES 2k Consortium, 2017. A global multiproxy database for temperature reconstructions of the Common Era. Scientific Data. 4, 170088. DOI: https://doi.org/10.1038/sdata.2017.88.

[38] PAGES 2k Consortium, 2019. Consistent multidecadal variability in global temperature reconstructions and simulations over the Common Era. Nature Geoscience. 12, 643–649. DOI: https://doi.org/10.1038/s41561-019-0400-0

[39] Levitus, S., Antonov, J., Boyer, T., 2005. Warming of the world ocean, 1955–2003. Geophysical Research Letters. 32, L02604. DOI: https://doi.org/10.1029/2004GL021592

[40] Feldman, D.R., Collins, W.D., Gero, P.J., et al., 2015. Observational determination of surface radiative forcing by CO_2 from 2000 to 2010. Nature. 519, 339–343. DOI: https://doi.org/10.1038/nature14240

[41] Shine, K.P., Cook, J., Highwood, E.J., et al., 2003. An alternative to radiative forcing for estimating the relative importance of climate change mechanisms. Geophysical Research Letters. 30(20), 2047. DOI: https://doi.org/10.1029/2003GL018141

[42] Loeb, N.G., Ham, S.-H., Allan, R.P., et al., 2024. Observational Assessment of Changes in Earth's Energy Imbalance since 2000. Surveys in Geophysics. DOI: https://doi.org/10.1007/s10712-024-09838-8

[43] Nikolov, N., Zeller, K.F., 2024. Roles of Earth's Albedo Variations and Top-of-the-Atmosphere Energy Imbalance in Recent Warming: New Insights from Satellite and Surface Observations. Geomatics. 4, 311–341. DOI: https://doi.org/10.3390/geomatics4030017

[44] ISCCP, International Satellite Cloud Climatology Project. See: Rossow, W.B., Duenas, E.N., 2004. The International Cloud Climatology Project (ISCCP). Bulletin of the American Meteorological Society. 85, 167–172.

[45] Zhang, Y., Rossow, W.B., 2023. Global radiative flux profile data set: Revised and extended. Journal of Geophysical Research: Atmospheres. 128, e2022JD037340. DOI: https://doi.org/10.1029/2022JD037340

[46] Taylor, P., 2009. Chill: a reassessment of global warming theory. Clairview: Forest Row, UK.

[47] Lockwood, M., Owen, M., Hawkins, E., et al., 2017.

Frost fairs, sunspots and the Little Ice Age. Astronomy & Geophysics. 58(2), 2.17–2.23. DOI: https://doi.org/10.1093/astrogeo/atx057
[48] Villalba, R., Lara, A., Masiokas, M.H., et al., 2012. Unusual Southern Hemisphere tree growth patterns induced by changes in the Southern Annular Mode. Nature Geosciences. 5, 793–798. DOI: https://doi.org/10.1038/ngeo 1613
[49] Abram, N.J., Mulvaney, R., Vimeux, F., et al., 2014. Evolution of the Southern Annular Mode during the past millennium. Nature Climate Change. 4, 564–569. DOI: https://doi.org/10.1038/nclimate2235
[50] Fletcher, M., Benson, A., Bowman, D.M.J.S., et al., 2018. Centennial-scale trends in the Southern Annular Mode revealed by hemisphere-wide fire and hydroclimatic trends over the past 2400 years Geological Society of America Data Repository item 2018. DOI: https://doi.org/10.1130/G39661.1
[51] Blunier, T., Brook, E.J., 2001. Timing of millennial-scale climate change in Antarctica and Greenland during the last glacial period. Science. 291, 109–112. Available from: http://www.fisica.edu.uy/~barreiro/papers/Blunier_etal_Science01.pdf
[52] Crucifix, M., 2012. Oscillators and relaxation phenomena in Pleistocene climate theory. Philosophical. Transactions of the Royal Society A Mathematics Physics Engineering Science. 370, 1140–1165. DOI: https://doi.org/10.1098/rsta.2011.0315
[53] Thompson, D.W.J.; Wallace, J.M., 1998. The Arctic Oscillation signature in the wintertime geopotential height and temperature fields Geophysical Research Letters. 25(9), 1297–1300. Available from: https://agupubs.onlinelibrary.wiley.com/doi/pdf/10.1029/98GL00950
[54] Polyakov, I.V., Bekryaev, R.V., Alekseev, G.V., et al. Variability and Trends of Air Temperature and Pressure in the Maritime Arctic, 1875–2000 Journal of Climate 2003, 16, 2067–2077. Available from: https://journals.ametsoc.org/view/journals/clim/16/12/1520-0442_2003_016_2067_vatoat_2.0.co_2.xml?tab_body=fulltext-display
[55] Polyarkov, I.V., Alekseev, G.V., Bekryaev, R.V., et al., 2001. Observationally based assessment of polar amplification of global warming. Geophysical Research Letters. 29, 1878. DOI: https://doi.org/10.1029/2001GL011111
[56] Park, W., Latif, M., 2008. Multi-decadal and multi-centennial variability of the meridional overturning circulation. Geophysical Research Letters. 35, L22703. DOI: https://doi.org/10.1029/2008GL035779
[57] van Oldenborgh, G.J., te Raa, L.A., Dijkstra, H.A., et al., 2009. Frequency- or amplitude-dependent effects of the Atlantic meridional overturning on the tropical Pacific Ocean. Ocean Sciences. 5(3), 293–301. DOI: https://doi.org/10.5194/os-5-293-2009
[58] Salinger, M.J., Renwick, J.A., Mullan, A.B., 2001. Inter-decadal Pacific Oscillation and South Pacific Climate. International Journal of Climatology. 21(14), 1705–1721. DOI: https://doi.org/10.1002/joc.691
[59] Meehl, G.A., Hu, A., Arblaster, J.M., et al., 2013. Externally forced and internally generated decadal climate variability associated with inter-decadal Pacific Oscillation. Journal of Climate. 26, 7298–7310. DOI: https://doi.org/10.1175/JCLI-D-12-00548.1
[60] Halpert, M.S., Ropelewski, C.F., 1992. Surface temperature patterns associated with the Southern Oscillation Journal of Climate. 5, 577–593.
[61] Li, J., Sun, C., Jin, F.-F., 2013. NAO implicated as a predictor of Northern Hemisphere mean temperature multidecadal variability. Geophysical Research Letters. 40, 5497–5502. DOI: https://doi.org/10.1002/2013GL057877
[62] Christy, J.R., McNider, R.T., 2017. Satellite Bulk Tropospheric Temperatures as a Metric for Climate Sensitivity Asia-Pacific Journal of Atmospheric Sciences. 53(4), 511–518. DOI: https://doi.org/10.1007/s13143-017-0070-z
[63] Bryden, H.L., Longworth, H.R., Cunningham, S.A., 2005. Slowing of the Atlantic meridional overturning circulation at 25º N. Nature. 438, 655–657. Available from: http://www.blc.arizona.edu/courses/schaffer/182h/Climate/AtlanticOverturning.pdf
[64] Bryden, H.L., King, B.A.; McCarthy, G.D., et al., Impact of a 30% reduction in Atlantic meridional overturning during 2009–2010. Ocean Science 2014, 10, 683–691. DOI: https://doi.org/10.5194/os-10-683-2014
[65] Smeed, D.A., Josey, S.A., Beaulieu, C., et al., 2018. The North Atlantic Ocean is in a state of reduced overturning. Geophysical Research Letters. 45, 1527–1533. DOI: https://doi.org/10.1002/2017GL076350
[66] Frajka-Williams, E., Ansorge, I.J., Baehr, J., et al., 2019. Atlantic Meridional Overturning Circulation: Observed Transport and Variability. Frontiers in Marine Science. 6, 260. DOI: https://doi.org/10.3389/fmars.2019.00260
[67] Chen, X., Tung, K.-K., 2014. Varying planetary heat sink led to global warming slowdown and acceleration. Science. 345, 897. DOI: https://doi.org/10.1126/science.1254937
[68] Latif, M., Martin, T., Reintges, A., et al., 2017. Southern Ocean Decadal Variability and Predictability Current Climate Change Reports. 3(3), 163–173. DOI: https://doi.org/10.1007/s40641-017-0068-8
[69] Meehl, G.A., Hu, A., Arblaster, J.M., et al., 2013. Externally forced and internally generated decadal climate variability associated with inter-decadal Pacific Oscillation. Journal of Climate. 26, 7298–7310. DOI:

https://doi.org/10.1175/JCLI-D-12-00548.1

[70] Trenberth, K.E., Caron, J.M., Stepaniak, D.P., et al., 2002. Evolution of El Niño Southern Oscillation and global atmospheric surface temperatures. Journal of Geophysical Research. 107(D8), 4065. DOI: https://doi.org/10.1029/2000JD000298

[71] Trenberth, K.E., Fasullo, J.T., 2009. Global warming due to increasing absorbed solar radiation. Geophysical Research Letters. 36, L07706. DOI: https://doi.org/10.1029/2009GL037527

[72] Keenlyside, N.S., Latif, M., Jungklaus, J., et al., 2008. Advanced decadal-scale climate prediction in the North Atlantic sector. Nature. 453, 84–88. DOI: https://doi.org/10.1038/nature06921

[73] Koutsoyiannis, D., Efstratiadas, A., Mamassis, N., et al., 2008. On the credibility of climate predictions. Hydrological Sciences–Journal–des Sciences Hydrologiques. 53(4), 671–684. Available from: https://www.tandfonline.com/doi/pdf/10.1623/hysj.53.4.671

[74] Koutsoyiannis, D., Mamassis, N., Christofides, A., et al., 2008. Assessment of the reliability of climate predictions based on comparisons with historical time series. EGU General Assembly, Geophysical Research Abstracts. 10, 09074. Available from: www.itia.ntua.gr/en/docinfo/850/

[75] Flato, G., Marotzke, J., Abiodun, B., et al., 2013. Evaluation of climate models. In Climate Change 2013: The Physical Science Basis. Contribution of Working Group I to the Fifth Assessment Report of the Intergovernmental Panel on Climate Change. pp. 741–866. Available from: https://pure.mpg.de/rest/items/item_1977534/component/file_3040450/content

[76] Eastman, R., Warren, S.G., Hahn, C.J., 2011. Variations in cloud cover and cloud types over the ocean from surface observations, 1954–2008. Journal of Climate. 24, 5914–5934.

[77] Pierce, J.R., 2017. Cosmic rays, aerosols, clouds, and climate: Recent findings from the CLOUD experiment, Journal of Geophysical Research – Atmosphere. 122. DOI: https://doi.org/10.1002/2017JD027475

[78] Wang, K.C., Dickinson, R.E., Wild, M., 2012. Atmospheric impacts on climatic variability of surface incident solar radiation Atmospheric Chemistry and Physics. 12, 9581–9592. Available from: https://acp.copernicus.org/articles/12/9581/2012/acp-12-9581-2012.pdf

[79] Wong, T., Wielicki, B.A., Lee, R.B., III, et al., 2006. Re-examination of the observed decadal variability of the earth radiation budget using altitude-corrected ERBE/ERBS nonscanner WFOV data. Journal of Climate. 19, 4028–4040. Available from: https://ntrs.nasa.gov/api/citations/20080014856/downloads/20080014856.pdf

[80] Serreze, M.C., Barry, R.G., 2011. Processes and impacts of Arctic amplification: a research synthesis, Global and Planetary Change. 77, 85–96. DOI: https://doi.org/10.1016/j.gloplacha.2011.03.004

[81] Schweiger, A.J., 2004. Changes in seasonal cloud cover over the Arctic seas from satellite and surface observations Geophysical Research Letters. 31, L2207. DOI: https://doi.org/10.1029/2004GL020067

[82] Walter, K., Graf, H.-F., 2005. The North Atlantic variability structure, storm tracks, and precipitation depending on the polar vortex strength Atmospheric Chemistry and Physics, European Geosciences Union. 5(1), 239–248. Available from: https://hal.archives-ouvertes.fr/file/index/docid/295595/filename/acp-5-239-2005.pdf (cited 3 July 2020).

[83] Francis, J.A., Hunter, E., 2006. New insight into the disappearing Arctic sea ice. EOS Transactions of the American Geophysical Union. 87, 509–511. Available from: https://agupubs.onlinelibrary.wiley.com/doi/pdf/10.1029/2006EO460001

[84] Bjune, A., Bakke, J., Nesje, A., et al., 2005. Holocene mean July temperature and winter precipitation in western Norway inferred from palynological and glaciological lake-sediment proxies. The Holocene. 15(2), 177–189. Available from: http://bora.uib.no/bitstream/handle/1956/2490/July%20temp.pdf?sequence=1&isAllowed=y (cited 3 July 2020).

[85] Bakke, J., Lie, Ø., Dahl, S.O., et al., 2008. Strength and spatial patterns of the Holocene wintertime westerlies in the NE Atlantic region. Global and Planetary Change. 60, 28–41. DOI: https://doi.org/10.1016/j.gloplacha.2006.07.030

[86] Dübal, H.-R., Vahrenholt, F., 2001. Radiative Energy Flux Variation from 2001–2020. Atmosphere. 12, 1297. DOI: https://doi.org/10.3390/atmos12101297

[87] Forster, P., Ramaswamy, V., Artaxo, P., et al., 2008. Changes in Atmospheric Constituents and in Radiative Forcing. In: Climate Change 2007: The Physical Science Basis. Contribution of Working Group I to the Fourth Assessment Report of the Intergovernmental Panel on Climate Change. Edited by Solomon, S. Cambridge University Press: Cambridge, UK; New York, NY, USA. Available from: https://www.ipcc.ch/site/assets/uploads/2018/02/ar4-wg1-chapter2-1.pdf

[88] Christiansen, B., 2002. Evidence for Nonlinear Climate Change: Two Stratospheric Regimes and a Regime Shift. Journal of Climate. 16, 3681. Available from: https://journals.ametsoc.org/jcli/article/16/22/3681/30043 (cited by 3 July 2020).

[89] Scafetta, N., Bianchini A., 2022. Planetary Theory of Solar Variability. Frontiers in Astronomy and Space Sciences. 9, 93793017. Available from: https://www.frontiersin.org/articles/10.3389/fspas.2022.937930

[90] Schindell, D.T., Rind, D., Balachandaran, N.,

et al., 1999. Solar cycle variability, ozone, and climate. Science. 284, 305–308. Available from: http://citeseerx.ist.psu.edu/viewdoc/download?doi=10.1.1.1012.6243&rep=rep1&type=pdf

[91] Schindell, D.T., Schmidt, G.A., Mann M.E., et al., 2001. Solar forcing of regional climate change during the Maunder Minimum. Science. 294 (5549), 2149–2152. Available from: https://ntrs.nasa.gov/archive/nasa/casi.ntrs.nasa.gov/20020049982.pdf

[92] Masson-Delmotte, V., Schultz M., 2013. Information from Paleoclimate Archives. In: Climate Change 2013: The Physical Science Basis. Contribution of Working Group I to the Fifth Assessment Report of the Intergovernmental Panel on Climate Change. Edited by Stocker, T.F. Cambridge University Press: Cambridge, UK; New York, NY, USA. Available from: https://www.ipcc.ch/site/assets/uploads/2018/02/WG1AR5_Chapter05_FINAL.pdf

[93] Ogurtsov, M.G., Nagovitsyn, Y.A., Kocharov, G.E., et al., 2002 . Long period cycles of the Sun's activity recorded in direct solar data and proxies. Solar Physics. (211), 371–394. Available from: https://www.researchgate.net/profile/M_Ogurtsov/publication/226593664_Long-Period_Cycles_of_the_Sun%27s_Activity_Recorded_in_Direct_Solar_Data_and_Proxies/links/00b7d52a74309e4c92000000.pdf

[94] Francis, J.; Vavrus, S.J., 2015. Evidence for a wavier jet stream in response to rapid Arctic warming. Environmental Research Letters. 10, 014005. DOI: https://doi.org/10.1088/1748-9326/10/1/014005

[95] Francis, J.A., Vavrus, S.J., Cohen, J., 2017. Amplified Arctic Warming and Mid-Latitude Weather: new perspectives on emerging connections. WIREs Wiley Interdisciplinary Reviews. 8(5), e474. DOI: https://doi.org/10.1002/wcc.474

[96] Wang, C., Yao, Y.L., Wang, H.L., et al., 2021. The 2020 summer floods and 2020/21winter extreme cold surges in China and the 2020 typhoon season in the western North Pacific. Advances in Atmospheric Sciences. 38(6), 896−904. DOI: https://doi.org/10.1007/s00376-021-1094-y

[97] Gillet, N.P., Stone D.A., Stott, P.A., et al., 2008. Attribution of polar warming to human influence. Nature Geoscience. 1(11), 750–754. DOI: https://doi.org/10.1038/ngeo338

[98] Blackport, R., Screen, J.A., 2020. Insignificant effect of Arctic amplification on the amplitude of midlatitude atmospheric waves. Science Advances. 6, eaay2880. Available from: https://www.science.org/doi/epdf/10.1126/sciadv.aay2880

[99] Vintner, B.M., Buchardt, S.L., Clausen, H.B., et al., 2009. Holocene thinning of the Greenland Ice Sheet. Nature. 461, 385−388. DOI: https://doi.org/10.1038/nature08355

[100] Lorenz, E.N., 2004. Designing chaotic models. Journal of Atmospheric Sciences. 62, 1574–1587. Available from: https://journals.ametsoc.org/view/journals/atsc/62/5/jas3430.1.xml?tab_body=pdf

[101] Eschenbach, W., 2023. Climate models and climate muddles. 2023. Available from: https://www.netzerowatch.com/content/uploads/2023/06/Eschenbach-Climate-Models.pdf

[102] Scafetta, N., 2012. Multi-scale harmonic model for solar and climate cyclical variation throughout the Holocene based on Jupiter–Saturn tidal frequencies plus the 11-year solar dynamo cycle. Journal of Atmospheric and Solar-Terrestrial Physics. 80, 296–311. Available from: https://arxiv.org/pdf/1203.4143.pdf

[103] Scafetta, N., 2013. Discussion on climate oscillations: CMIP5 general circulation models versus a semi-empirical harmonic model based on astronomical cycles. Earth-Science Reviews. 126, 321–357. DOI: https://doi.org/10.1016/j.earscirev.2013.08.008

[104] Scafetta, N., Bianchini, A., 2023. Overview of the Spectral Coherence between Planetary Resonances and Solar and Climate Oscillations. Climate. 11, 77. DOI: https://doi.org/10.3390/cli11040077

[105] Connolly, R., Soon, W., Connolly, M., et al., 2021. How much has the Sun influenced Northern Hemisphere temperature trends? An ongoing debate. Astronomy and Astrophysics. Available from: https://arxiv.org/abs/2105.12126https://www.sciencedirect.com/science/article/pii/S1674987123001172?via%3Dihub (cited 14 July 2023).

[106] Charvatova, I., 2009. Long term predictive assessments of solar and geomagnetic activities made on the basis of close similarities between solar interial motion in the interval 1840–1905 and 1980–2045. New Astronomy. 14, 25–30. Available from: http://files.klimaskeptik.cz/200001060891438a1e7/charvatova%202009%20newastronomy.pdf

[107] Stefani, F., 2021. Solar and Anthropogenic Influences on Climate: Regression Analysis and Tentative Predictions. Climate. 9, 163. DOI: https://doi.org/10.3390/cli9110163

[108] Davis, W.J., 2023. Mass extinctions and their relationship with atmospheric carbon dioxide concentration: Implications for Earth's future. Earth's Future. 11, e2022EF003336. DOI: https://doi.org/10.1029/2022EF003336

[109] Jackson, T., Taylor, P., 1992. The precautionary principle and the prevention of marine pollution Chemistry and Ecology. 7(1–4), 123–134. DOI: https://doi.org/10.1080/02757549208055436

[110] Symes, M., 2024. Exploring options for actively cooling the Earth, Version 2, 2024. ARIA – Advanced Research and Invention Agency, London, UK. Available from: https://www.aria.org.uk/wp-content/uploads/2024/05/AR

IA-Actively-cooling-the-earth-programme.pdf

[111] Asadi, M., Azordeh Molkabadi, S., Engameh, S., 2024. The Amine-Functionalized MCM-41 for Hydration and Utilization of CO_2. Pollution. 10(1), 374–382. DOI: https://doi.org/10.22059/POLL.2023.362270.1992

[112] Davis, W.J., 2017. The Relationship between Atmospheric Carbon Dioxide Concentration and Global Temperature for the Last 425 Million Years Climate. 5(4), 76. DOI: https://doi.org/10.3390/cli5040076